Icarus **159**, 369–395 (2002)
doi:10.1006/icar.2002.6907

Models of Twenty Asteroids from Photometric Data

M. Kaasalainen, J. Torppa, and J. Piironen

Observatory, University of Helsinki, P.O. Box 14, FIN-00014 Helsinki, Finland
E-mail: Mikko.Kaasalainen@astro.helsinki.fi

Received October 6, 2001; revised February 18, 2002

We present models of the shapes and rotational states of selected asteroids based on data from the Uppsala Asteroid Photometric Catalogue. The results show a wide variety of shapes especially among the smaller asteroids. Few asteroids show clear signs of significant albedo variegation. Most rotational states are in reasonable agreement with those previously estimated with rough models. We discuss some practical aspects of photometric analysis and present a simple way of building one-spot models.

Key Words: **asteroids, rotation; photometry; surfaces, asteroids.**

1. INTRODUCTION

Disk-integrated photometric data are a major source of information on the physical properties of asteroids. If a set of lightcurves measured at various observing geometries is available, an asteroid's global shape and its rotational state, as well as the basic photometric characteristics of its surface, can be robustly determined (Kaasalainen and Torppa 2001, hereafter KT; Kaasalainen *et al*. 2001).

After over fifty years of observations, there is now an abundance of photoelectric lightcurve data. About 10,000 lightcurves of several hundred objects have been measured so far, but the lack of a universally acknowledged standard data base still remains a practical problem. To date, the only collection of lightcurves aiming at completeness is the Uppsala Asteroid Photometric Catalogue (UAPC), now in its fifth and last version under the present title and format (Lagerkvist *et al*. 2001) (for a printed copy of UAPC, please contact `classe@astro.uu.se`). This catalogue was succesfully used in Kaasalainen *et al*. (2001) when comparing lightcurve inversion models with those obtained from radar or space probe observations. This prompted us to start analyzing the whole of the Uppsala Catalogue; the first results of this survey are described in this paper, shortly to be followed by more. We estimate that the existing lightcurves already facilitate the general modeling of at least several tens of asteroids—almost all of those that have been preliminarily modeled with traditional techniques during the past half-century of modern observations.

The asteroids selected for this paper represent a sample of well-observed targets, picked from different parts of the UAPC without any particular bias. Most of these are, of course, main-belt asteroids: There are not yet many well-observed near-Earth asteroids (NEAs). However, in some cases the quickly changing observing geometries of NEAs make it possible to gather a good data set during just one apparition or two, so we expect the portion of NEA models to increase in the next few years.

To elucidate some facts of lightcurve inversion in a concise form, we ask and answer some "Frequently Asked Questions" in Section 2. In Section 3, we describe some practical aspects of the observational data and the modeling procedure. Section 4 contains the models for 3 Juno, 7 Iris, 10 Hygiea, 15 Eunomia, 16 Psyche, 20 Massalia, 22 Kalliope, 29 Amphitrite, 32 Pomona, 39 Laetitia, 43 Ariadne, 45 Eugenia, 52 Europa, 87 Sylvia, 192 Nausikaa, 354 Eleonora, 532 Herculina, 1036 Ganymed, 3103 Eger, and 6053 1993BW3. We sum up in Section 5.

2. LIGHTCURVE INVERSION FAQs

To summarize and emphasize what lightcurve inversion can and cannot do, we discuss some central points here in the form of questions (Q) and answers (A).

Q: What does "global shape" mean in terms of resolution? Is it something one would see from some distance away?

A: Roughly that. However, the model images from lightcurve inversion should not be regarded as "snapshots". Lightcurves simply do not contain information on small-scale shape details, so the model is as much a qualitative as a quantitative representation. Some of the intermediate-scale features of the inversion model are inevitably only suggestive of the real ones.

Q: Is it possible to resolve concave features?

A: Not usually. Any nonconvex model always portrays too much detail. Most nonconvex regions can equally well be modeled with suitable flat regions, and different versions of local indentations or bulges of the surface would give very similar lightcurves. Only very sizable nonconvexities, such as those of distinctly double-lobed contact (or separate and synchronous) binaries, can be inferred with some reliability.

Q: Is it possible to resolve albedo variegation?

A: Only partially. One can model a probable albedo spot, if there is clear evidence of albedo variegation (see Appendix). Attributing brightness variation to shape as much as possible

0019-1035/02 $35.00

gives the most stable solution. Lightcurves measured at various wavelengths may help in inferring potential albedo variegation.

Q: How many apparitions are needed for a model?

A: Three or four apparitions are usually sufficient for a decent model, given that they are observed at different ecliptic latitudes and longitudes; even one or two may suffice if the observing geometries vary considerably during an apparition.

Q: How many lightcurves does that mean?

A: If the data are very good, about 10 lightcurves (densely covering the whole rotation period) will already do. We have built good models from less than 20 "ordinary" lightcurves.

Q: Are large ($>30^\circ$) solar phase angles necessary?

A: No, but they are naturally very useful. Lightcurves with phase angles around 20° already provide good separation from the near-opposition geometry.

Q: How accurate must the lightcurves be?

A: Reasonably, but not especially accurate. Random noise of less than, say, 0.05 mag is no problem, especially if there are many points in a lightcurve. Systematic errors (affecting lightcurve shape and timing) carry much more weight than random ones.

Q: Is relative photometry sufficient?

A: Yes, for the shape/spin solution. Proper determination of scattering characteristics requires several lightcurves with well-defined absolute brightnesses.

Q: Is the observation wavelength important?

A: Only for detailed light-scattering analysis. Since relative photometry is sufficient for general modeling, one can easily use lightcurves measured with different filters.

3. OBSERVATIONAL DATA AND MODELING PROCEDURE

Despite being an excellent collection of lightcurve data, our data source, the UAPC, suffers from a number of drawbacks. Most of these problems can be traced back to the observer–catalogue interface: For example, some data have been received in formats that are very difficult to interpret. Another problem is that the data have usually been checked only partly or not at all. Some of the lightcurves are simply faulty for whatever reasons (often taken during bad weather conditions or even twilight), while some entries are incompletely or erroneously filled (sometimes the reported epochs refer to the local afternoon!), or blighted by ambiguous composite lightcurves. It is usually almost impossible to correct such errors afterward. This is why systematic errors are much more troublesome than random ones. Also, the formats used in the UAPC are unfortunately somewhat cumbersome and insufficiently standardized, easily leading to errors in automatic file handling. The use of the data base still requires a large amount of handwork.

3.1. Absolute and Relative Photometry

The foremost manifestation of the aforementioned problems is perhaps the poorly reported reliability of absolute magnitudes. In most cases it is hard to ascertain which lightcurve magnitudes can be considered at least close to absolute: Some are clearly relative (and reported to be such), some are probably absolute, while a number of lightcurves could be the one or the other.

Even if it is clear which lightcurves can be considered absolute and which relative, the fundamental truth of photometric observations remains unaltered: As every lightcurve observer knows (or should know), errors in the absolute magnitude (as a scale coefficient for a whole lightcurve) are usually at least as large as lightcurve noise. This just cannot be helped much: Accurate determination of the absolute brightness would require constant observation of a few good standard stars very close to the asteroid. Indeed, we have found that absolute lightcurve fits are always significantly worse than relative ones because they are inevitably more or less offset in brightness. The larger the offset, the more there is room for the lightcurve fit to deviate from the actual lightcurve shape in an attempt to close the gap. Making the offset shifts a posteriori would be hindsight rather than optimization. Thus it is simply not very practical to do absolute fitting: The model line can be flexibly fitted over the observed points only when using relative brightnesses.

Even when not very accurate, the absolute magnitudes contain essential information that can well be extracted with suitable regularization. For example, when using the Hapke scattering model (Bowell *et al*. 1989), the scale factors (i.e., the average brightness of the points of an observed lightcurve divided by that computed from the corresponding model points) of each absolute lightcurve are required to remain as close to constant as possible: The deviations give the offset errors of the observed absolute magnitudes. Such regularization is described in Kaasalainen *et al*. (2001); it makes sure that one finds the shape, pole, and scattering parameters that (1) accurately reproduce the shapes of the lightcurves and (2) give as much credit to the observed absolute magnitudes as possible while not spoiling item 1. This is also statistically sound because the more systematic errors of the absolute magnitudes are considered separate from those of the basically random relative ones.

3.2. Scattering Law and Stability

The absolute magnitudes are the richest source of information on the scattering law. On the other hand, as described in Kaasalainen *et al.* (2001) (and also checked for these models), the shape/spin model remains very much the same even when the parameters of the scattering model are changed somewhat, or if the form of the scattering law is changed altogether, as long as the parameters and laws describe roughly similar photometric properties. This has its curses and blessings: While the shape/spin solution is quite stable and separate, it also follows that multi-parameter scattering laws always have a region of ambiguous inverse solutions in the parameter space. Trying to pin down the best solution accurately can be a rather trying if not futile exercise with models such as the full Hapke one, unless (1) the allowed parameter region is strongly constrained,

(2) the absolute magnitudes are accurate, and (3) a wide range of the solar phase angle is covered. We also know that no current scattering law is exactly correct as they all are more or less crude approximations of the surface structure. This introduces another systematic error component.

In view of these problems, we have chosen to present here the shapes and rotational states of the selected targets, while the more detailed analysis of the scattering properties, being a somewhat separate topic, is left to another paper combining the results from a larger number of asteroids and discussing light-scattering models, phase curves and their definitions, etc. at greater length. For the purposes of the present paper, we used a few reliable-looking absolute magnitudes that could be found in each set. With these, we could check that, e.g., the (loose) parameter values used in the full Hapke model were consistent with both the observed magnitudes and the values customarily assigned to the corresponding classes of asteroids (Bowell *et al.* 1989, Helfenstein and Veverka 1989). The shapes and spin solutions presented here are thus not exactly the same as those corresponding to the eventual best-fit scattering models, but we know that the fine-tuning of the scattering parameters will not affect the spin/shape solutions appreciably. Any differences will be negligible compared to the actual differences between the model and the real shape/spin.

4. MODELS

We used convex modeling in all cases as no better fits could be obtained with nonconvex shapes (mostly because the convex fits were already excellent). The convex model does not overestimate the level of detail in the shape solution and keeps the attention in the global shape. The convex shape can be obtained with either a smooth function series or a large set of separate facet values (see KT); the former is an efficient tool when determining the rotation parameters. It is advisable to check the solution using both methods, as the end results may differ somewhat (especially when the number of lightcurves or observing geometries is limited) since the parameter sets have very different sizes. It is best to start the iteration from a spherical initial shape in both cases: This makes the results independent of other models or guesses. The separate facet set may sometimes seem to display details that are too small to be inferred from lightcurves, whereas the smooth function series may occasionally exaggerate some global features in a caricature-like fashion. In any case, the shape result must always be interpreted as much qualitatively as quantitatively.

Large flat areas seen on the convex models usually indicate potential nonconvexities such as indentations or large craters. This is why the convex version should not be taken as a "solid" model of homogeneous density: The corresponding inertia tensor could be incorrect. Thus it does not matter if the model seems to be rotating around a slightly wrong axis. We have found the spin/shape information contained in the lightcurves to be so robust that the shape solution is automatically quite consistent with the requirement of relaxed rotation (for actually precessing asteroids see Kaasalainen 2001). This requirement is not a very strong (i.e., informative) constraint for the shape in general, but if nonconvex modeling is tried, it should be used as one regularizing tool.

For each asteroid, we show a simple mugshot-type pair of images, some 90° apart in longitude and seen from the equatorial level. We also show four typical lightcurve fits for each; α is the solar phase angle, and θ and θ_0 are the aspect angles of, respectively, the Earth and the Sun. The very approximate relative triaxial dimensions of each object are reported as the numbers a/b and b/c. Since such dimensions cannot be determined unambiguously, we use the mean values of two definitions. One is given by placing the a-axis along the azimuthal direction of the longest extent of the body, and determining the b and c extents accordingly; the other is given by finding the ellipsoid that minimizes the $\Delta\rho$ that gives the difference between two convex bodies (Kaasalainen *et al.* 2001). In both cases the c-axis coincides with the vertical z-axis (i.e., the rotation axis) of the inversion result.

The scattering models used for these asteroids were the five-parameter Hapke law (with parameters fixed or confined to the typical value regimes) and the one introduced in Kaasalainen *et al.* (2001). Both gave very similar results; the shape differences are smaller than the expected differences between the real and depicted shapes. When using relative photometry, an interesting fact is that variations within the Hapke parameters usually have very little effect on the shape as long as they remain inside realistic values. (It is just the scale factors, mentioned in Section 3.1, that show different patterns.) It is precisely this property that prompted us to introduce the simple empirical scattering model of Kaasalainen *et al.* (2001). A typical effect of changing the scattering law from, e.g., the Hapke model to the empirical one is the occasional slight uniform flattening of the shape result (less than 10%) while the body still looks much the same, as if the image had been slightly distorted in the vertical direction. This is a quite natural effect of relative photometry, for the mere shapes of lightcurves obviously tend to constrain the a/b dimension of the shape of the body more strongly than the b/c one, especially if the set of observational polar aspects is limited.

In Table I, we list some characteristic properties of the twenty asteroids. These are the ecliptic latitude and longitude (β and λ, J2000) of the rotation axis, the sidereal rotation period in hours, the observation span of the input data, the number N_a of apparitions observed, the solar phase angle range and total number N_{lc} of lightcurves, and the rms deviation of the relative lightcurve fit (in magnitudes). N_a gives an idea of the number of different observing geometries; however, some apparitions occurred in quite similar geometries, and for some only one or two lightcurves of varying quality were observed. Typically roughly half of the input lightcurves were strictly relative; i.e., either no absolute magnitude value was quoted or it was clearly unreliable. The aspect angle range for both the Sun and the

TABLE I
Parameters for 20 Asteroids

Asteroid	β	λ	Period (h)	Obs. yrs.	N_a	α range	N_{lc}	rms Δ (mag)
3 Juno	+27°	103°	7.209531	1954–91	10	1°–30°	27	0.009
7 Iris	+10°	20°	7.138841	1950–91	13	4°–29°	32	0.018
10 Hygiea	−30°	115°	27.62321	1953–91	10	1°–16°	18	0.013
	−30°	300°						
15 Eunomia	−65°	355°	6.082752	1950–95	13	3°–27°	31	0.031
16 Psyche	−9°	35°	4.195947	1955–92	19	1°–21°	85	0.016
	−2°	216°						
20 Massalia	+45°	10°	8.097714	1955–92	6	0°–27°	18	0.018
	+45°	189°						
22 Kalliope	−21°	20°	4.148200	1953–86	13	1°–22°	24	0.013
	+6°	197°						
29 Amphitrite	−21°	138°	5.390119	1962–86	11	1°–24°	27	0.010
32 Pomona	+58°	267°	9.447669	1965–89	6	1°–24°	18	0.033
39 Laetitia	+35°	323°	5.138237	1949–88	21	5°–23°	46	0.020
43 Ariadne	−15°	253°	5.761986	1965–90	8	2°–30°	32	0.024
45 Eugenia	−30°	124°	5.699143	1969–88	9	1°–23°	44	0.017
52 Europa	−57°	79°	5.631610	1976–94	6	1°–11°	16	0.012
87 Sylvia	+66°	71°	5.183642	1978–89	8	3°–17°	32	0.045
192 Nausikaa	−7°	306°	13.62254	1963–85	3	2°–28°	19	0.017
354 Eleonora	+20°	356°	4.277180	1954–87	10	1°–23°	16	0.021
532 Herculina	+10°	289°	9.404951	1954–92	9	4°–24°	40	0.010
1036 Ganymed	−76°	208°	10.312	1985–89	2	6°–55°	21	0.014
3103 Eger	−50°	10°	5.706772	1986–97	4	14°–45°	13	0.044
6053 1993 BW3	−8°	358°	2.5739	1995–96	1	5°–75°	19	0.026
	+10°	178°						

Note. β and λ are, respectively, the ecliptic latitude and longitude of the pole (J2000); "Obs. yrs." gives the length of the total observation span; N_a denotes the number of observed apparitions; "α range" gives the range of the solar phase angle in the observations; N_{lc} denotes the number of lightcurves; and "rms Δ" is the rms deviation of the model fit.

Earth covered both "hemispheres" quite well for these asteroids. The error estimates for the pole coordinates vary slightly; we can just as well use a bulk error of some $\pm 5^\circ$ for both latitude and longitude unless otherwise stated. Similarly, the period error varies in accordance with the lengths of the period and the observation span (and subspans); we quote the periods such that the error estimate is roughly of the order of the last unit digit.

The publications containing the observations and potential previous models of these asteroids are listed in the UAPC (see also the fourth and earlier updates). Our spin state solutions and rough triaxial dimensions agree reasonably well with most previous estimates, though the pole differences can be several tens of degrees (which is inevitable for the many asteroids that cannot even be approximated by an ellipsoid). It should also be remembered that most earlier models are based only on a small subset of the lightcurves we used for any given asteroid. If our pole solution was very different from an earlier model, we double-checked that the latter solution was not a good one accidentally overlooked by us.

For scaling purposes, we quote the approximate IRAS estimate of each asteroid's diameter (see, e.g., Small Bodies Data Archives: `http://pdssbn.astro.umd.edu/sbnhtml/index.html#asteroids`); we also state their taxonomic classes.

3 Juno (Figs. 1 and 2). Juno (S-type, 240 km) is apparently a very regular, equilibrium-like body, roughly characterized by dimensions $a/b = 1.2,\ b/c = 1.3$. The adopted pole solution was clearly the best one: Mirror versions cannot fit the lightcurves as well.

7 Iris (Figs. 3 and 4). Iris (S-type, 200 km) is a rather roughly cut spherical body, characterized by $a/b = 1.2,\ b/c = 1.0$. We cannot rule out the mirror solution $\lambda + 180^\circ$, although the adopted one (and particularly the corresponding shape solution) seems more consistent. The data set available was not a very good one, suffering from bad timings, ambiguous composites, etc. There are some albedo effects, so probably some of the rough cuts seen in the images should be attributed to albedo markings (a flat large facet corresponding to a brighter albedo spot, and a sharper edge corresponding to a darker region—see KT). A single-spot albedo model is probably not sufficient here.

10 Hygiea (Figs. 5 and 6). Hygiea (C-type, 430 km) has a very long period, so only a small part of the period can be covered during one night. This does not preclude a good solution, but a twofold ambiguity remains in the pole result as

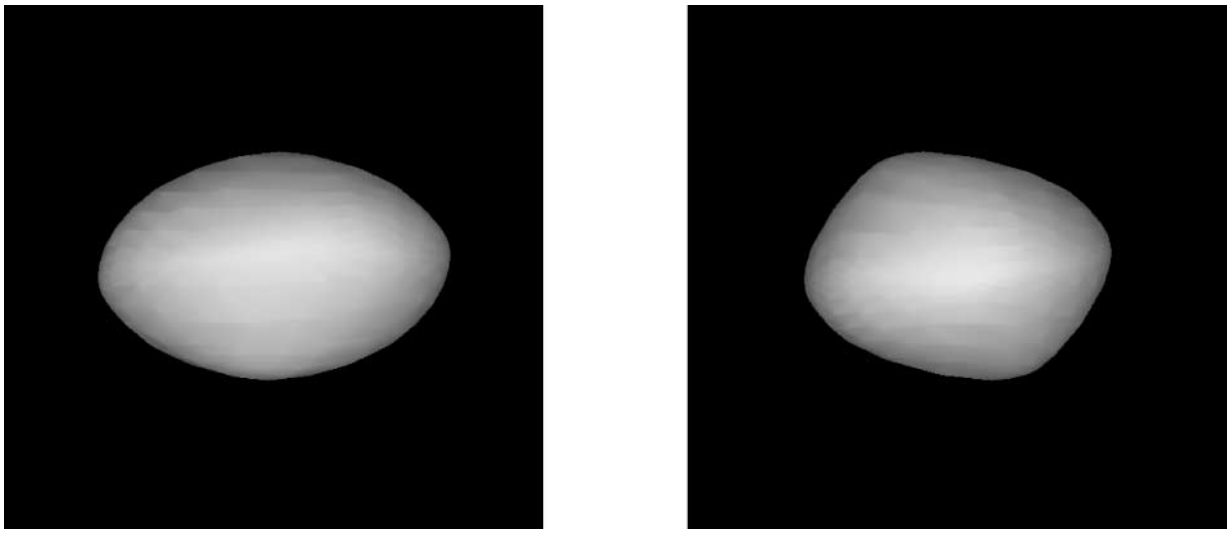

FIG. 1. The shape model of 3 Juno, shown at equatorial viewing/illuminaton geometry, with rotational phases 90° apart.

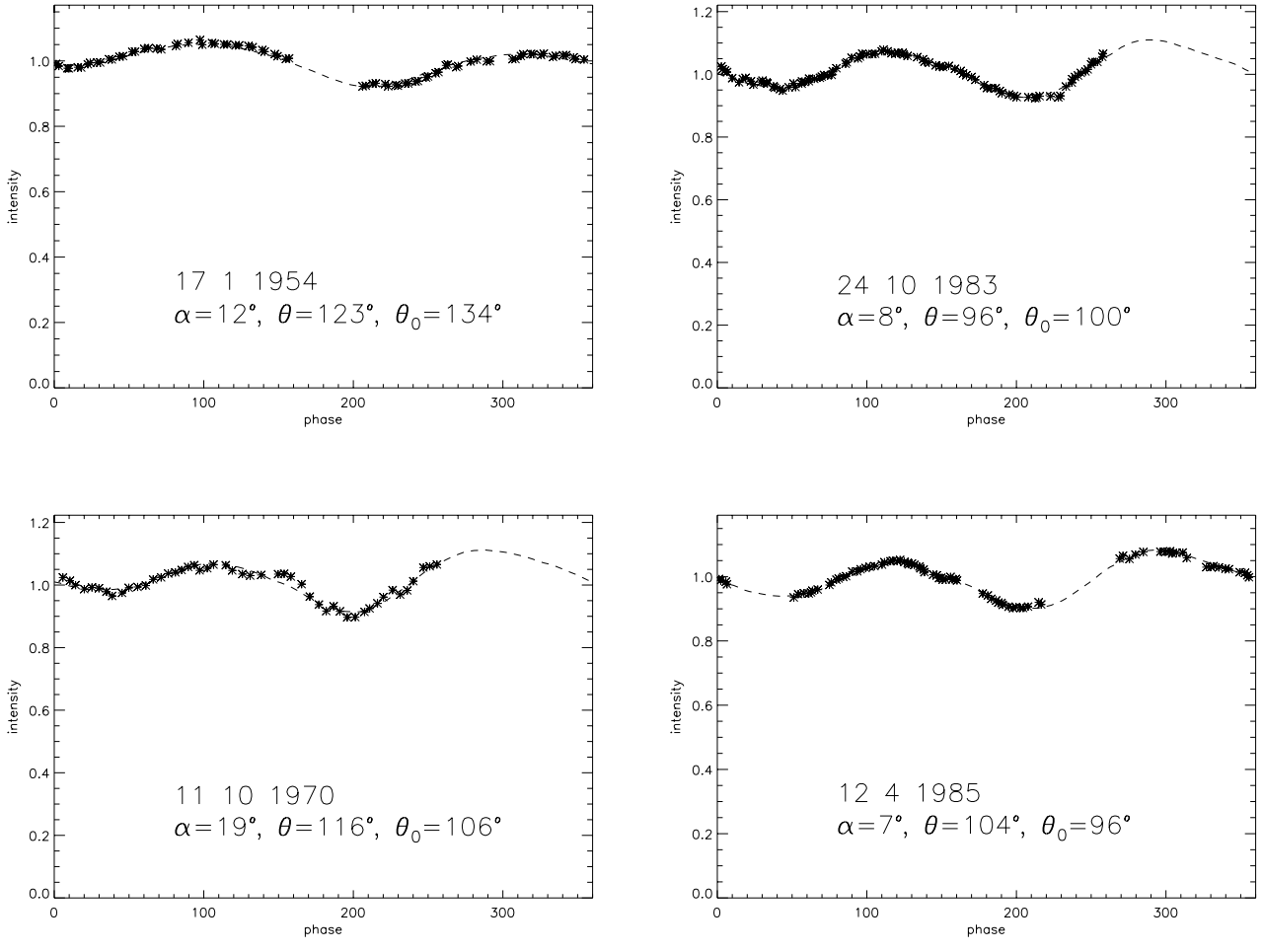

FIG. 2. Four lightcurves (asterisks) and the corresponding fits (dashed lines) for 3 Juno. The rotational phase is given in degrees, and the brightness in units of relative intensity. The aspect angle of the Earth (measured from the North pole) is given by θ, and that of the Sun by θ_0. The solar phase angle is given by α.

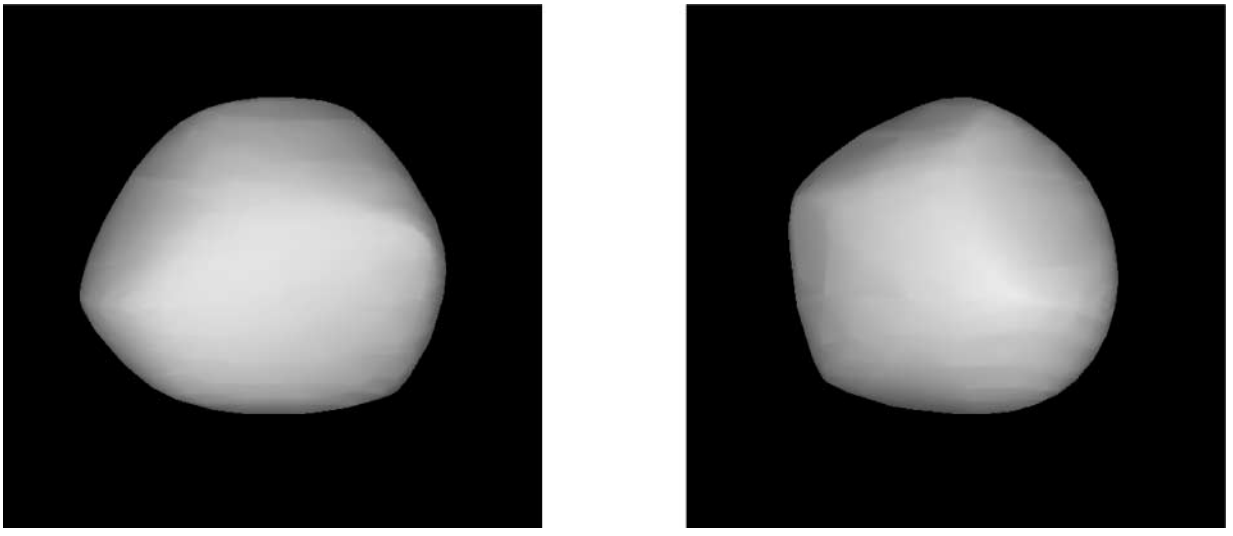

FIG. 3. The shape model of 7 Iris.

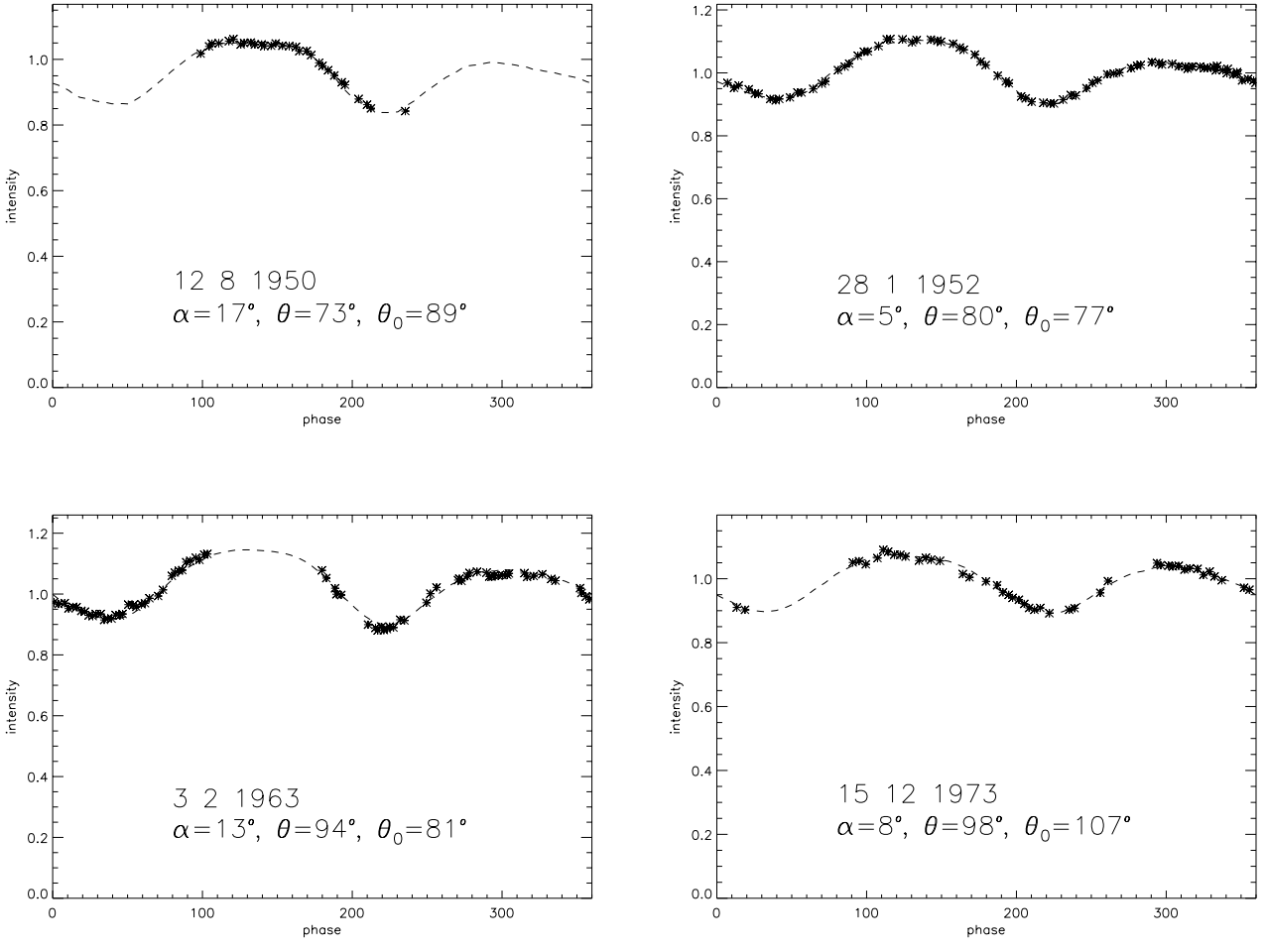

FIG. 4. Four lightcurves and the corresponding fits for 7 Iris.

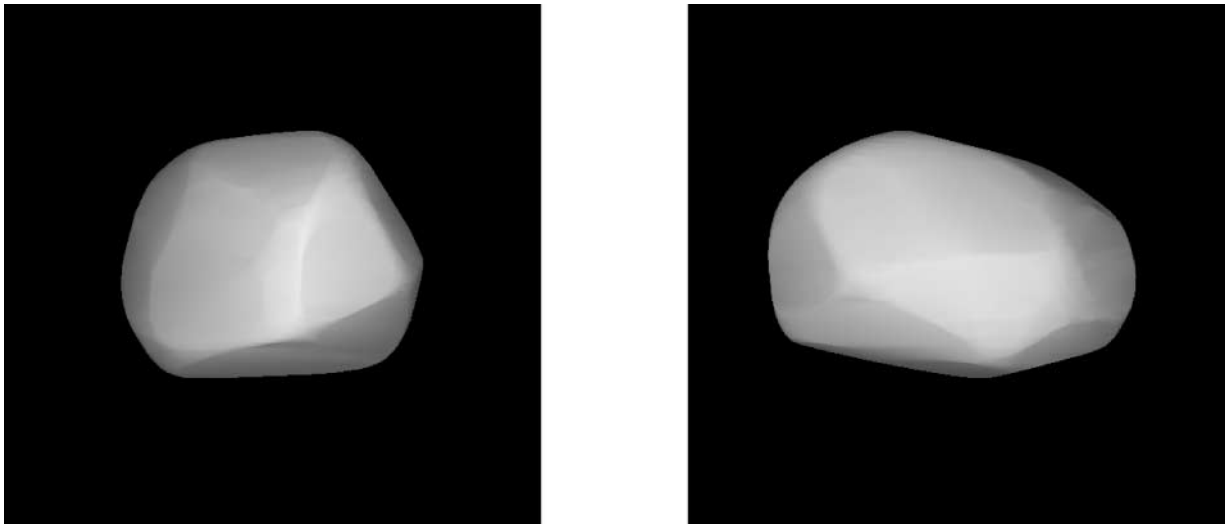

FIG. 5. The shape model of 10 Hygiea.

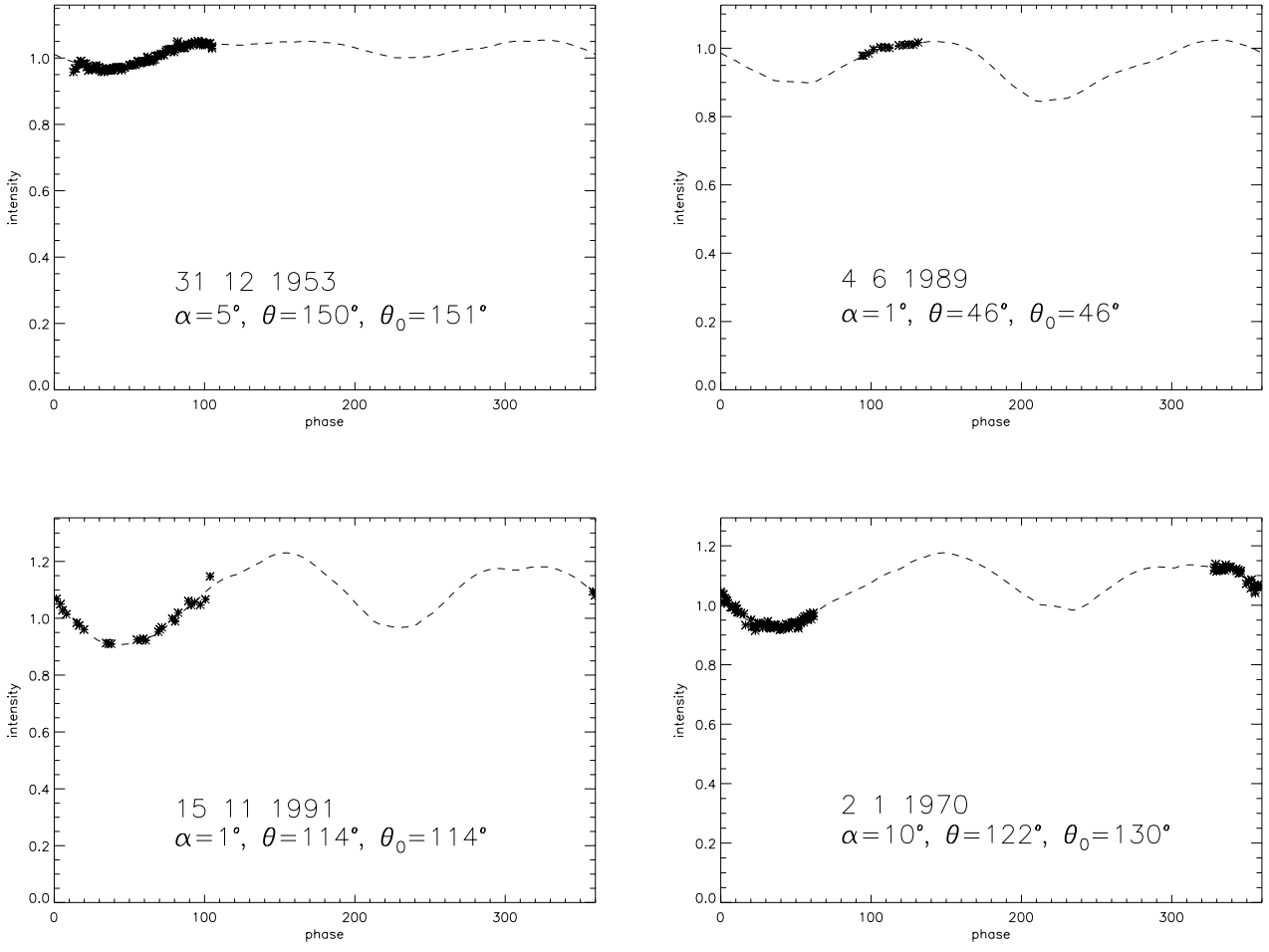

FIG. 6. Four lightcurves and the corresponding fits for 10 Hygiea.

Hygiea moves close to the plane of the ecliptic. The shape results ($a/b = 1.3,\ b/c = 1.1$) are very similar for the same reason.

15 Eunomia (Figs. 7 and 8). Eunomia (S-type, 270 km) is a very regular, quasi-ellipsoidal object with dimensions $a/b = 1.4$, $b/c = 1.2$. The adopted pole was clearly the best one; for example, there is a pole possibility at some $\lambda = 110^\circ$ giving a decent fit, but the corresponding shape fit would be completely unrealistic, implying rotation about a wrong principal inertia axis.

16 Psyche (Figs. 9 and 10). Psyche (M-type, 260 km) is a rather regular body with roughly $a/b = 1.2$, $b/c = 1.2$. Two pole solutions gave equally good fits; the corresponding shape solutions are very similar (roughly mirror images of each other). The residual vector (1) of the Appendix clearly indicated albedo variegation, and this was subsequently modeled with a bright-spot feature of moderate size (on the long side opposite to the one shown in Fig. 9) some 30% brighter than the rest of the surface. We do not show the spot model here as its probable location and strength are really all that can be inferred with any reliability from photometry alone—any rendering would probably be misleading.

20 Massalia (Figs. 11 and 12). Massalia (S-type, 150 km) also remains close to the ecliptic, so we have two pole solutions with the shape characterized by $a/b = 1.1, b/c = 1.1$. The shape is quite spherical, and the lightcurve features are explained by large planar, nonconvex parts of the surface.

22 Kalliope (Figs. 13 and 14). Kalliope's (M-type, 190 km) recently discovered satellite (Margot and Brown 2001, Merline and Menard 2001) does not seem to have a visible effect on the lightcurves. Two pole solutions are possible, with shape dimensions of roughly $a/b = 1.2$, $b/c = 1.2$. The $\lambda = 197^\circ$ pole, however, produced a visibly smaller scale factor scatter among the lightcurves with reliable absolute magnitudes, so it is the more probable candidate.

29 Amphitrite (Figs. 15 and 16). Amphitrite (S-type, 220 km) is almost spherical with rough dimensions $a/b = 1.1$, $b/c = 1.1$. The adopted pole solution gave the best fit, and there were no obvious rivaling pole regions.

32 Pomona (Figs. 17 and 18). Pomona (S-type, 80 km) is quite an angular object, with $a/b = 1.3$, $b/c = 1.1$. The adopted pole solution clearly gave the best fit, and the shape model was physically the most consistent. Some of the lightcurves were very noisy (at and above 0.05 mag), but we used them as well since the total number of lightcurves was less than 20.

39 Laetitia (Figs. 19 and 20). Laetitia (S-type, 160 km) is a rather irregular body, with no indication of significant albedo variegation. Its rough dimensions are $a/b = 1.4$, $b/c = 1.4$. Again, the adopted pole solution was clearly superior to other possibilities.

43 Ariadne (Figs. 21 and 22). Ariadne (S-type, 70 km) is an elongated and slightly angular body without prominent albedo markings. The crude dimensions are $a/b = 1.6$, $b/c = 1.2$. The chosen pole gave the best fit and had no apparent rivals.

45 Eugenia (Figs. 23 and 24). Eugenia's (C-type, 210 km) small satellite Petit-Prince (Merline *et al.* 1999) does not have any effect on the lightcurves as its projected area is less than half a percent of that of the primary. Eugenia is a rather elongated and roughly cut body, with crude dimensions $a/b = 1.4$, $b/c = 1.5$ and no signs of albedo variegation.

52 Europa (Figs. 25 and 26). Europa (C-type, 310 km) is a rather well-behaved, regular body with dimensions roughly $a/b = 1.2$, $b/c = 1.2$. The mirror pole at $\beta = -44^\circ$, $\lambda = 246^\circ$ cannot be completely ruled out as it gives as good a fit, but the chosen one produces a more realistic shape solution: The mirror one would include an irregular bulge not probable in a body of this size. In any case, the model cannot be better than crude for two reasons: (1) the solar phase angles are low, and (2) the already scarce data are contaminated by composite lightcurves over many days (and several degrees of solar phase angle). Low solar phases emphasize the symmetric shape part of the body, so there is not much information available on asymmetric features. The practice of forming composite lightcurves very easily destroys valuable information, so it should only be applied with extreme caution and preferably not at all.

87 Sylvia (Figs. 27 and 28). Despite its large size, Sylvia (C-type, 270 km) seems to be a somewhat angular, irregular body. Its very crude dimensions are $a/b = 1.4$, $b/c = 1.1$. As with 22 Kalliope and 45 Eugenia, its small satellite (Brown and Margot 2001) does not show in the lightcurves. The adopted pole solution was physically the most plausible: The mirror pole at $\beta = +52^\circ$, $\lambda = 293^\circ$ gives as good a fit, but the corresponding shape would rotate around a wrong principal inertia axis.

192 Nausikaa (Figs. 29 and 30). The long-period asteroid Nausikaa (S-type, 110 km) is roughly cut but not very elongated ($a/b = 1.3, b/c = 1.1$). The ecliptic latitude of the pole solution is not very well confined; its accuracy is some $\pm 10^\circ$. The mirror solution $\beta = +36^\circ$, $\lambda = 131^\circ$ (with a very similar shape model) cannot be completely ruled out with the existing data set, but the adopted pole direction gives the most consistent fit.

354 Eleonora (Figs. 31 and 32). Eleonora (S-type, 160 km) is quite a regular body with roughly $a/b = 1.2$, $b/c = 1.1$. The adopted pole solution stood out as the one producing the most consistent shape and fit; however, its accuracy cannot be much better than $\pm 10^\circ$.

532 Herculina (Figs. 33 and 34). The convex model of Herculina (S-type, 230 km) resembles a toaster. The large planar areas indicate nonconvexities, probably large craters à la Mathilde; the approximate dimensions are $a/b = 1.1, b/c = 1.2$. Our data base contained many obviously garbled lightcurves, but the abundant good ones clearly indicated the adopted pole solution as the best one. The interesting features of the lightcurves (such as the changing number of maxima and minima) can easily be explained with this shape (cf. Golevka in Kaasalainen *et al.* 2001). No significant albedo variegation was indicated.

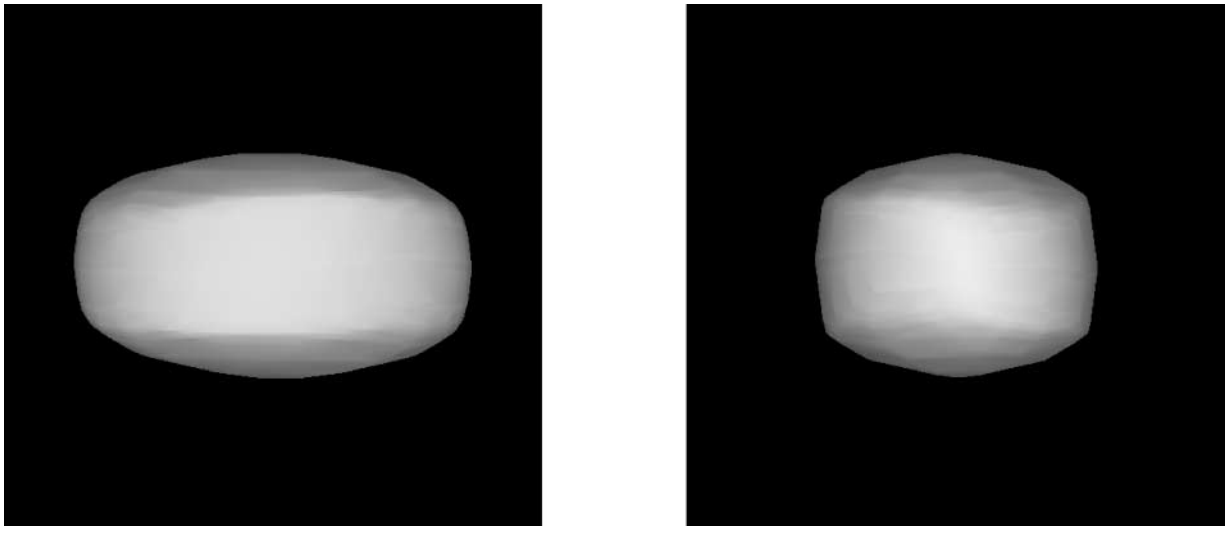

FIG. 7. The shape model of 15 Eunomia.

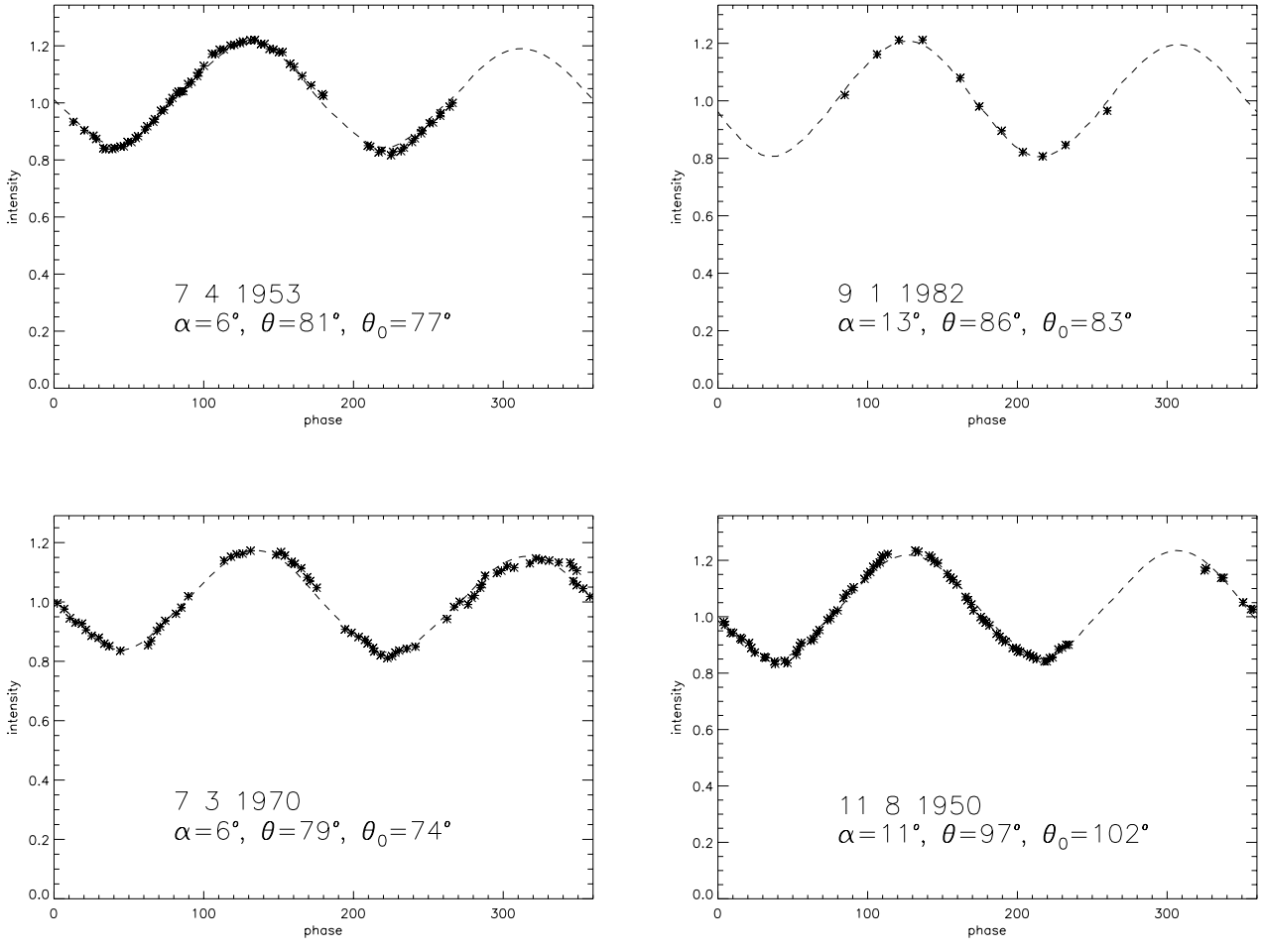

FIG. 8. Four lightcurves and the corresponding fits for 15 Eunomia.

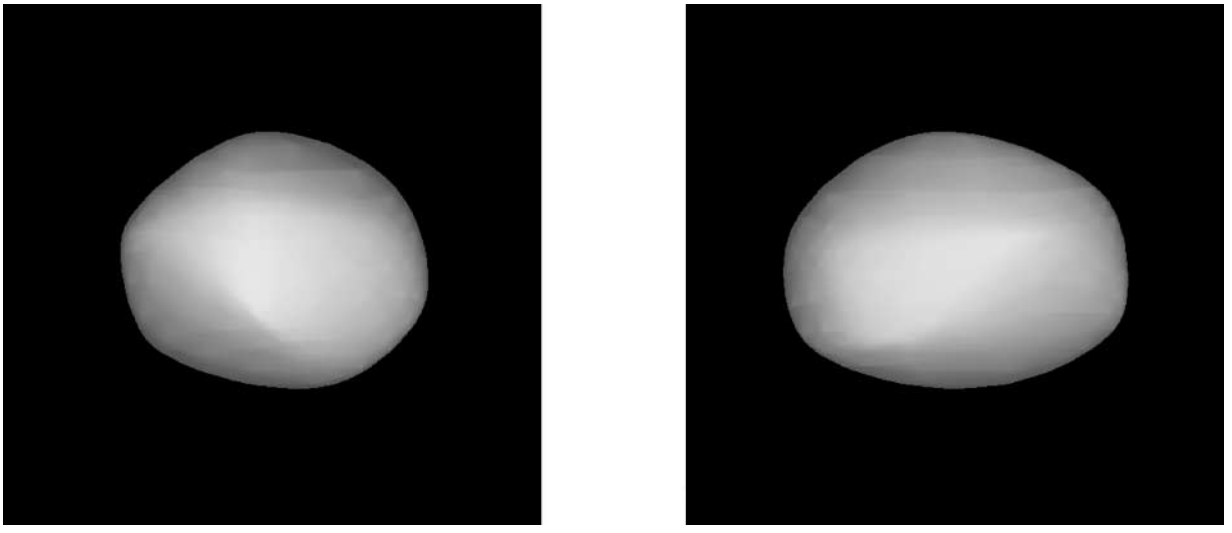

FIG. 9. The shape model of 16 Psyche.

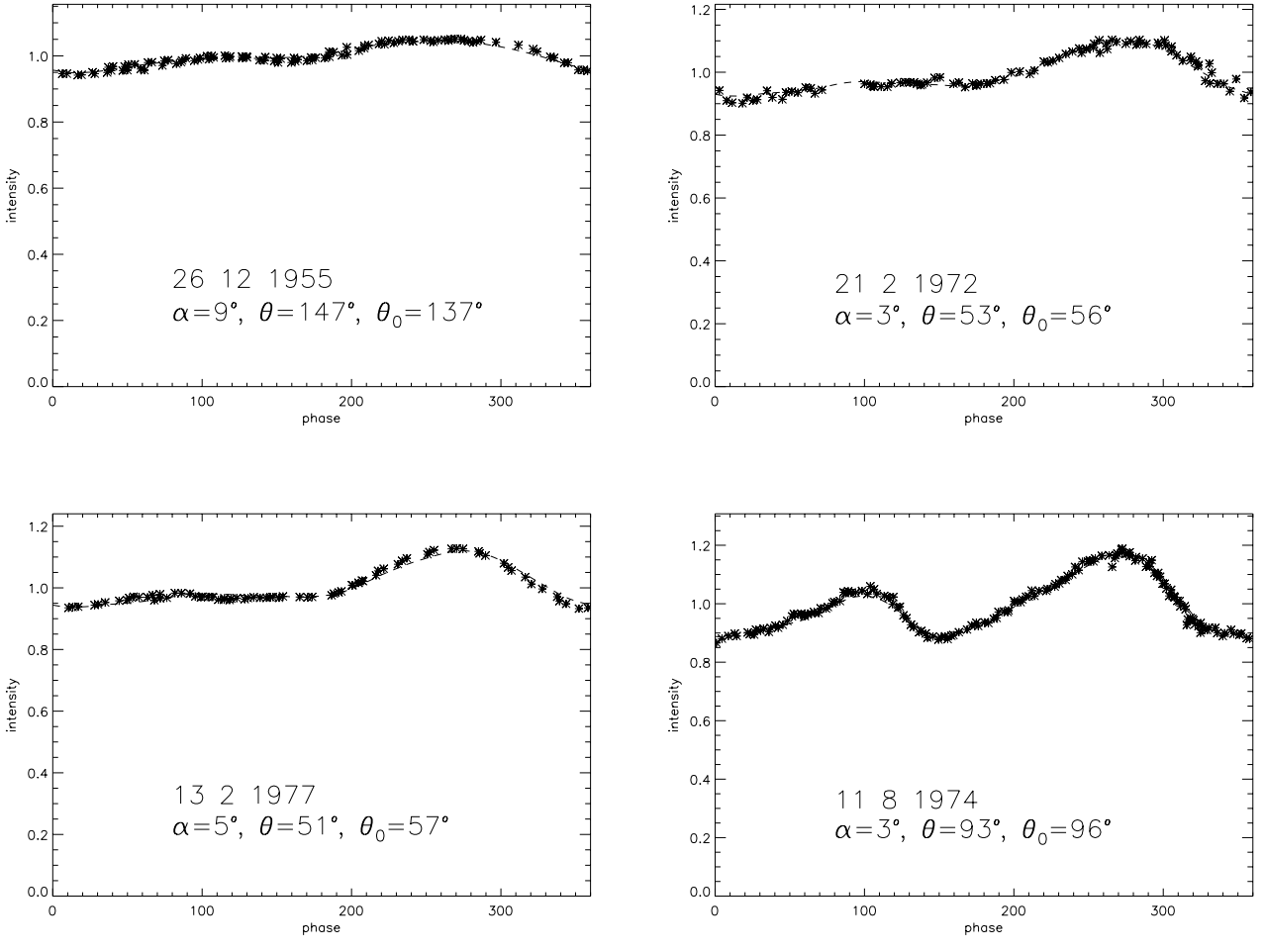

FIG. 10. Four lightcurves and the corresponding fits for 16 Psyche.

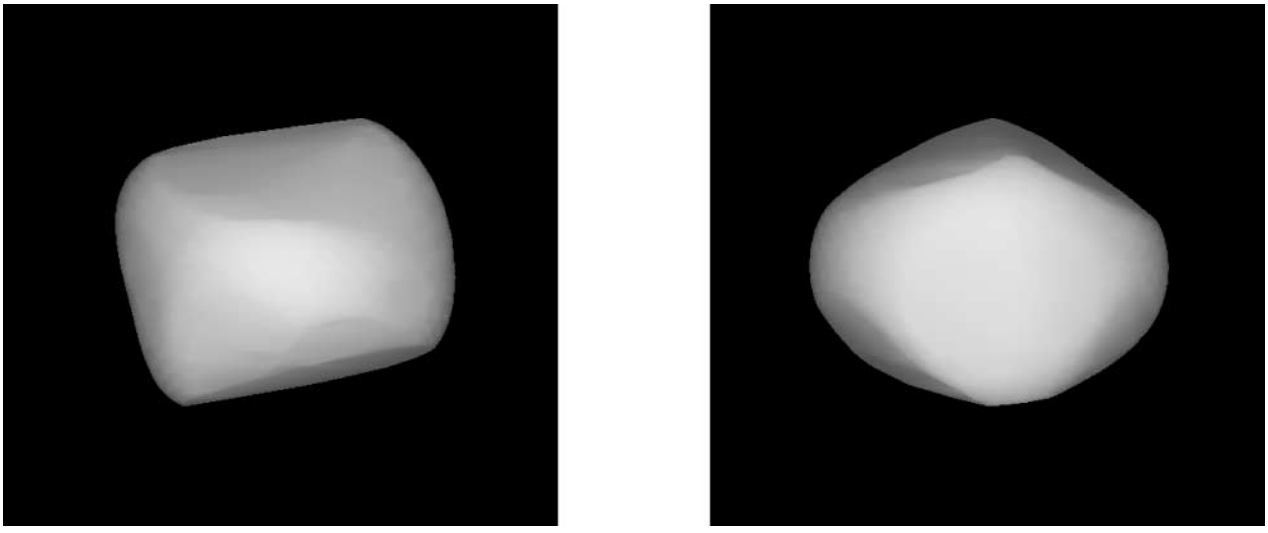

FIG. 11. The shape model of 20 Massalia.

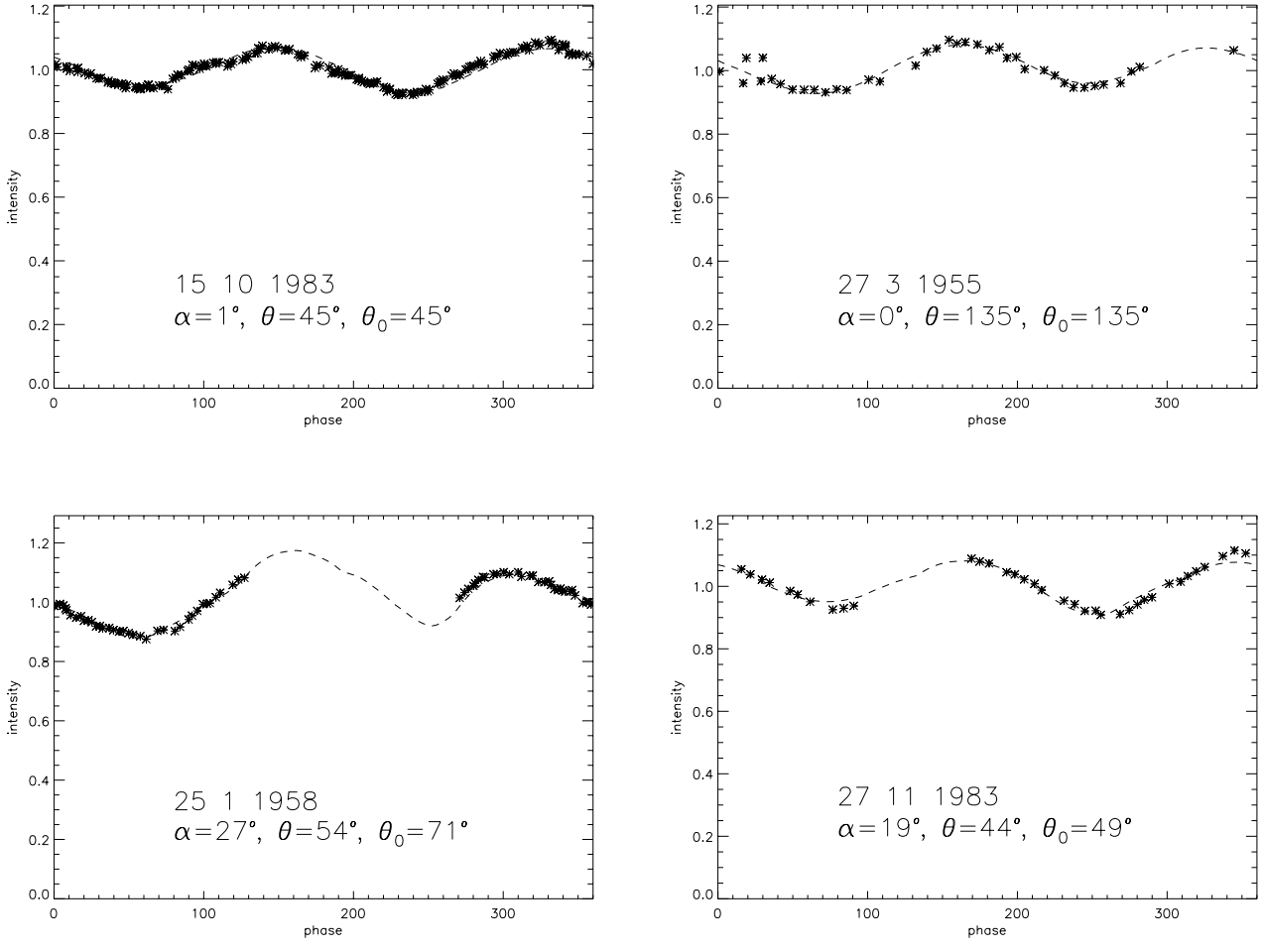

FIG. 12. Four lightcurves and the corresponding fits for 20 Massalia.

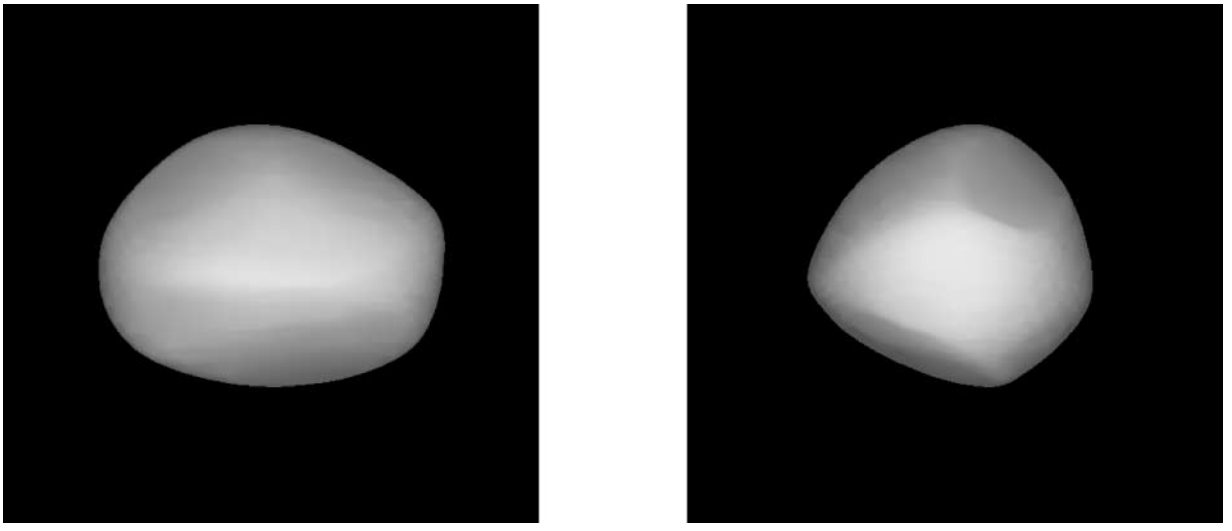

FIG. 13. The shape model of 22 Kalliope.

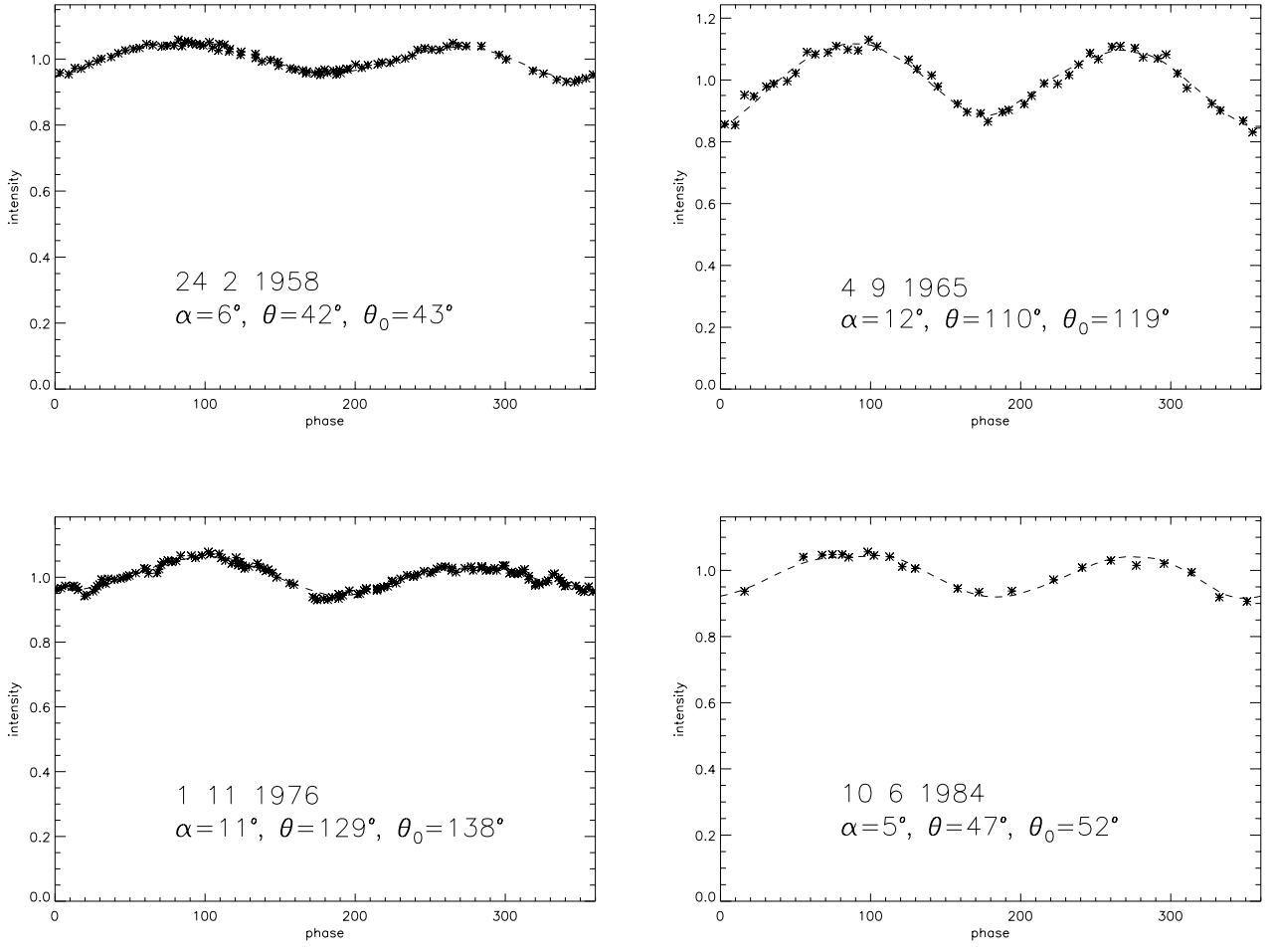

FIG. 14. Four lightcurves and the corresponding fits for 22 Kalliope.

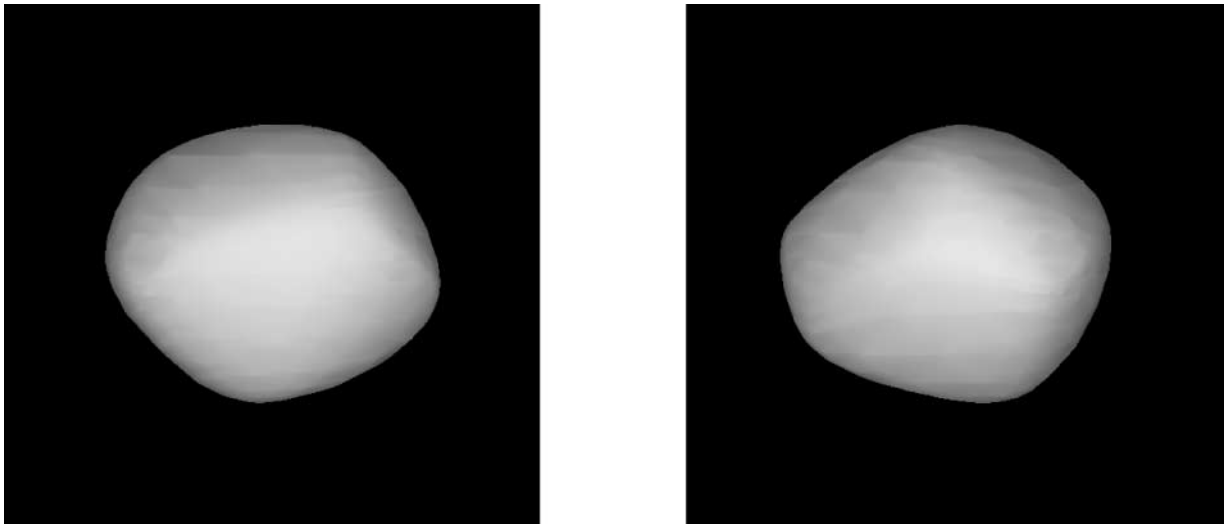

FIG. 15. The shape model of 29 Amphitrite.

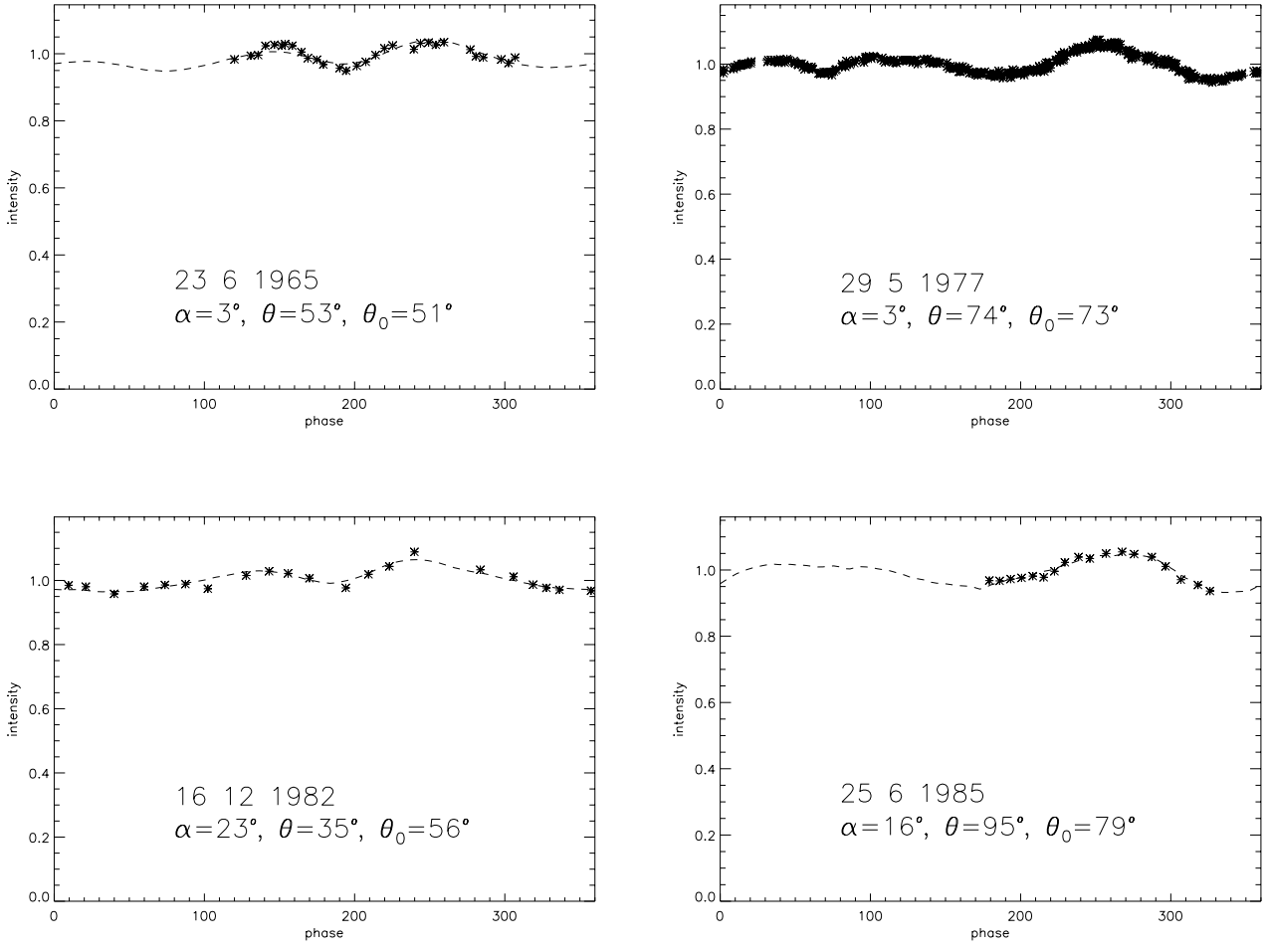

FIG. 16. Four lightcurves and the corresponding fits for 29 Amphitrite.

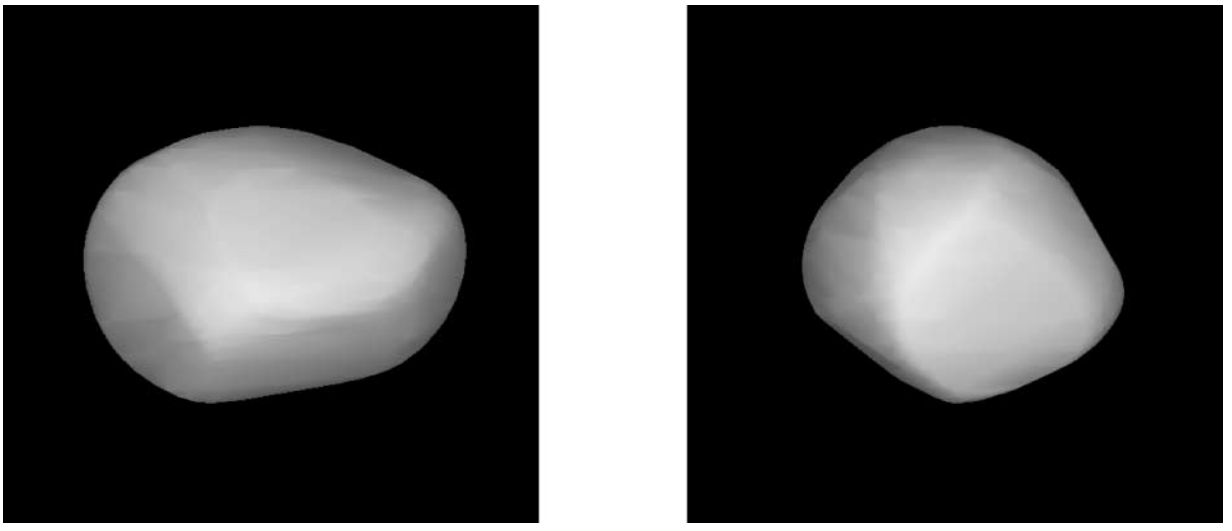

FIG. 17. The shape model of 32 Pomona.

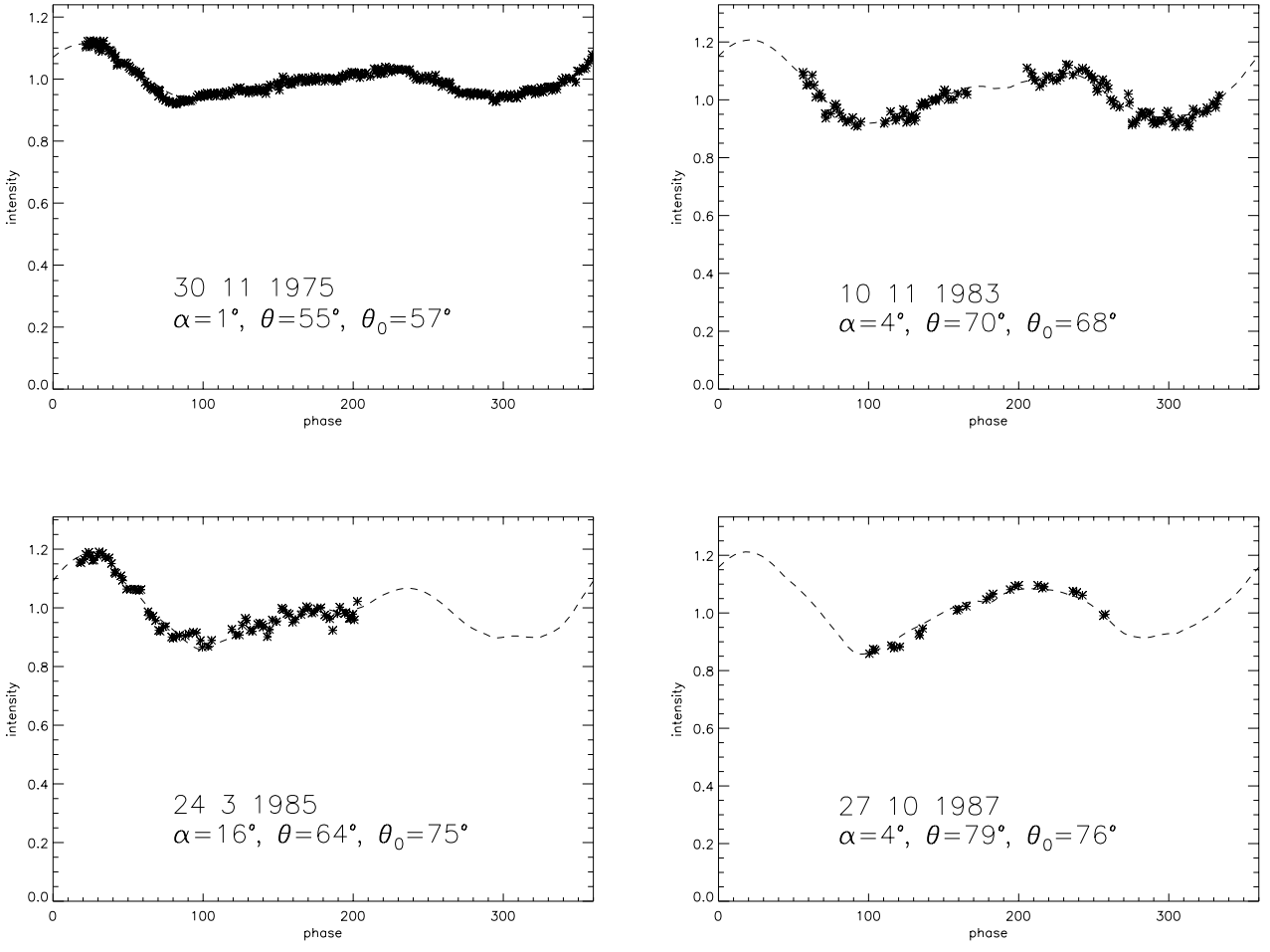

FIG. 18. Four lightcurves and the corresponding fits for 32 Pomona.

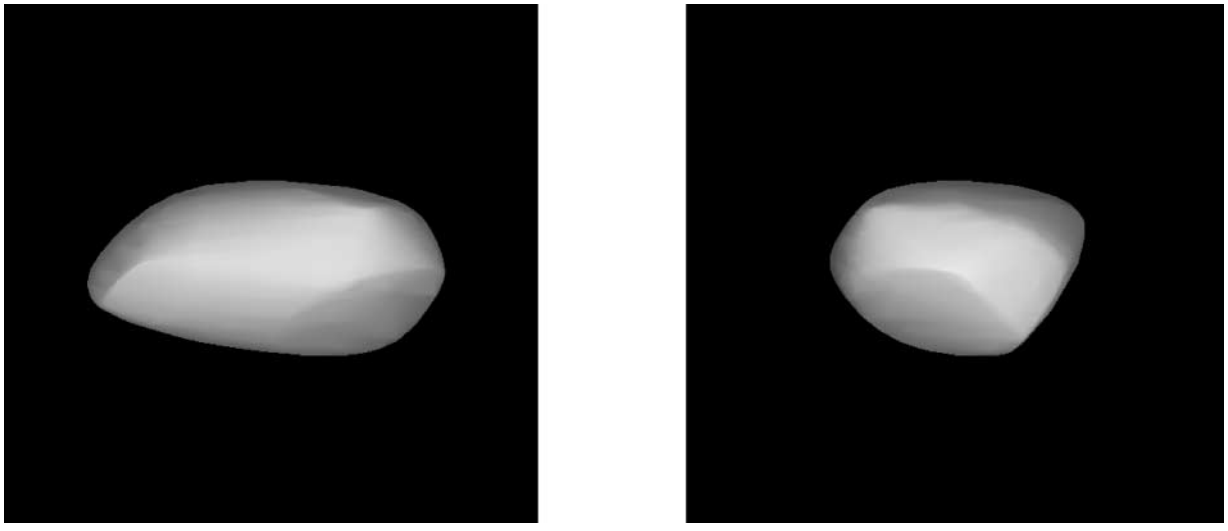

FIG. 19. The shape model of 39 Laetitia.

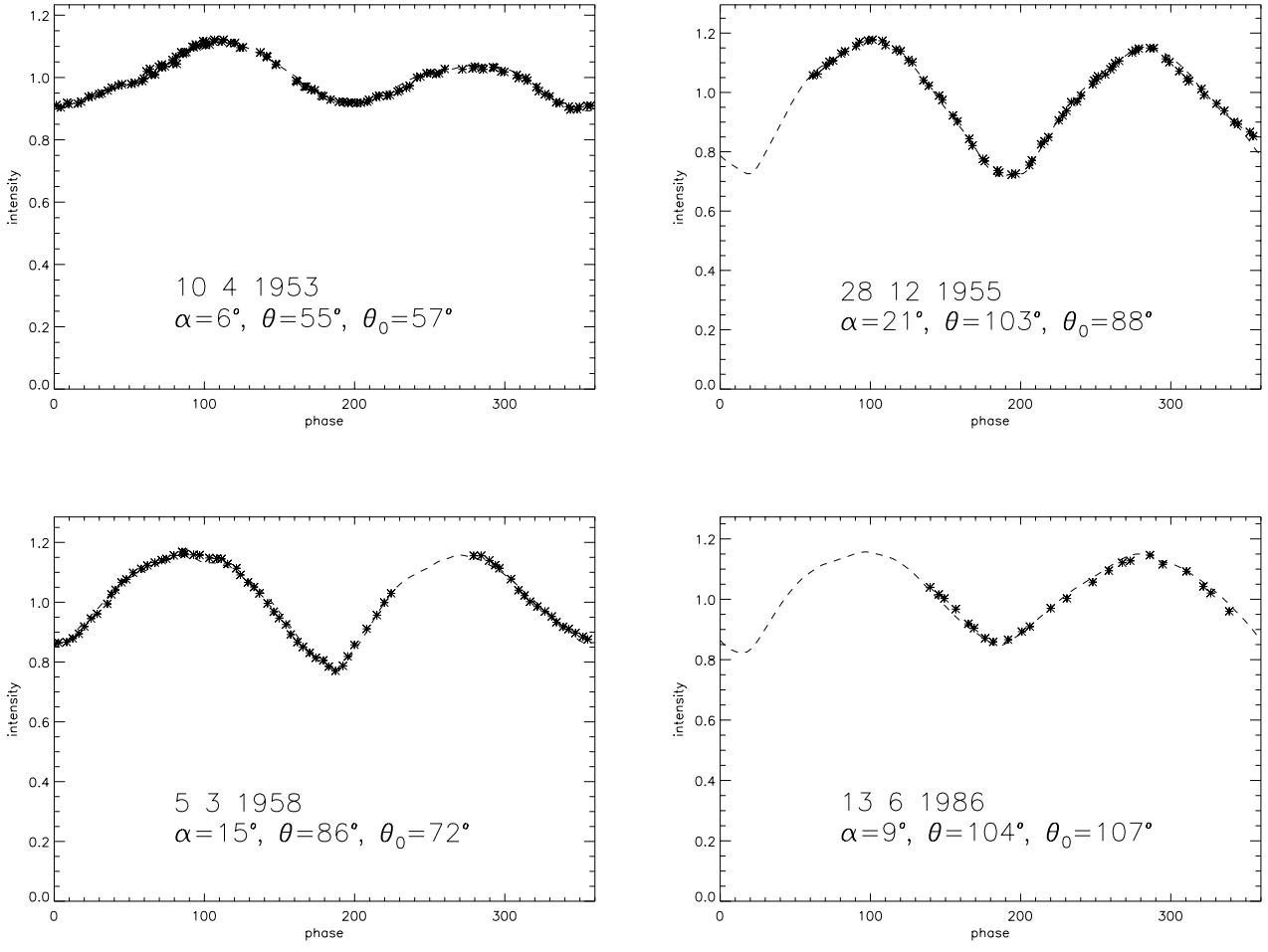

FIG. 20. Four lightcurves and the corresponding fits for 39 Laetitia.

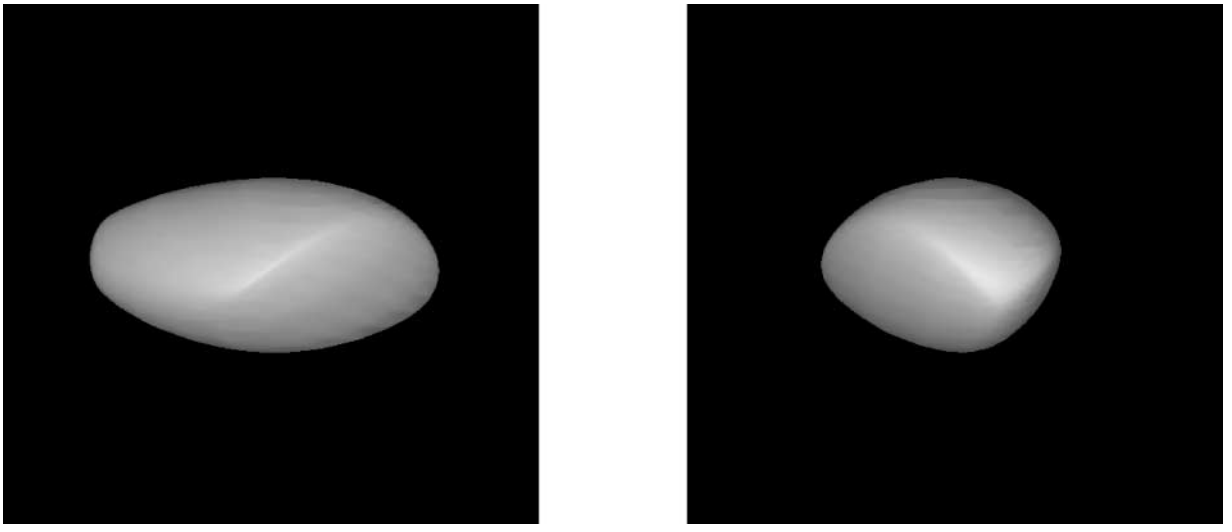

FIG. 21. The shape model of 43 Ariadne.

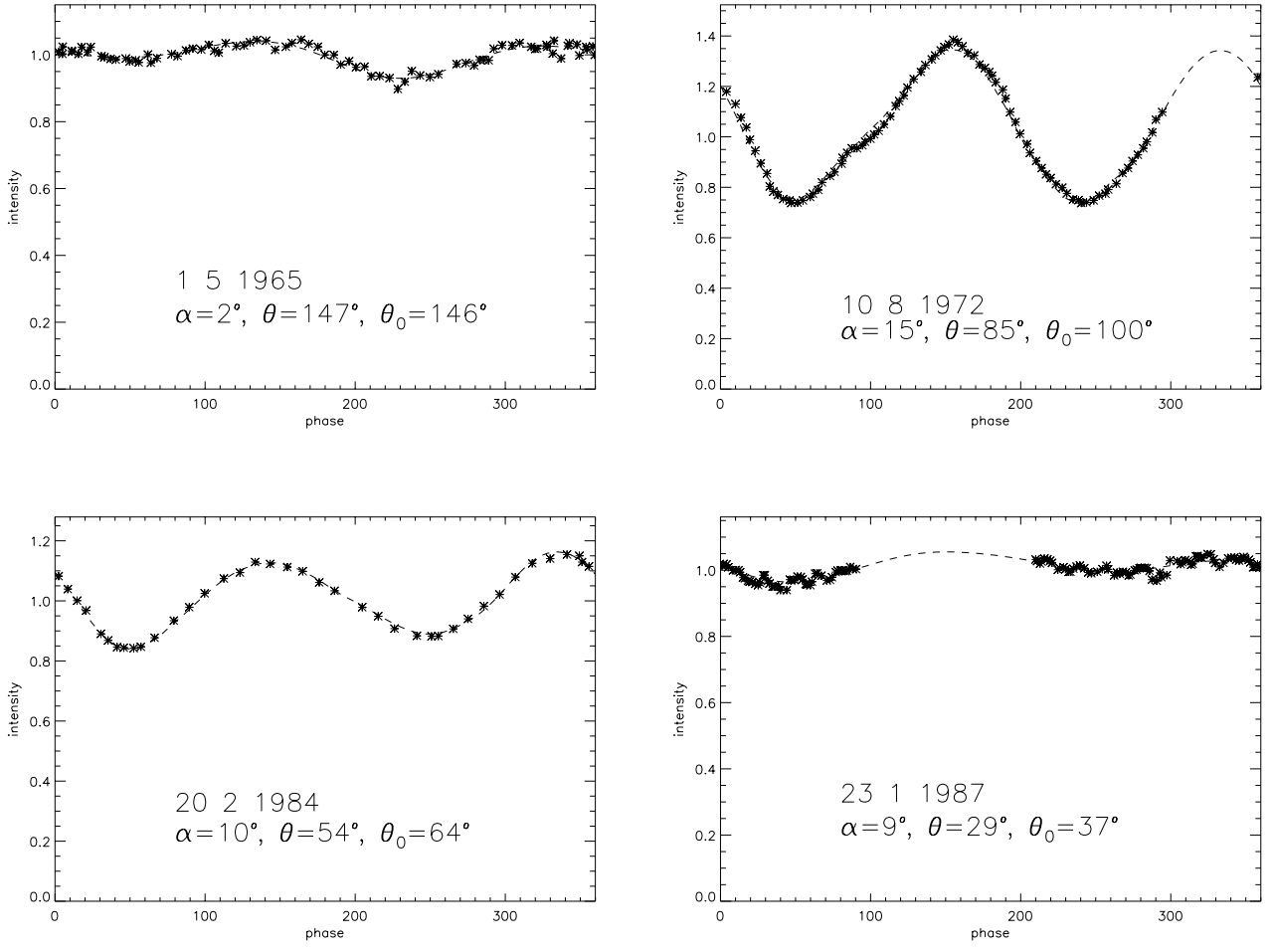

FIG. 22. Four lightcurves and the corresponding fits for 43 Ariadne.

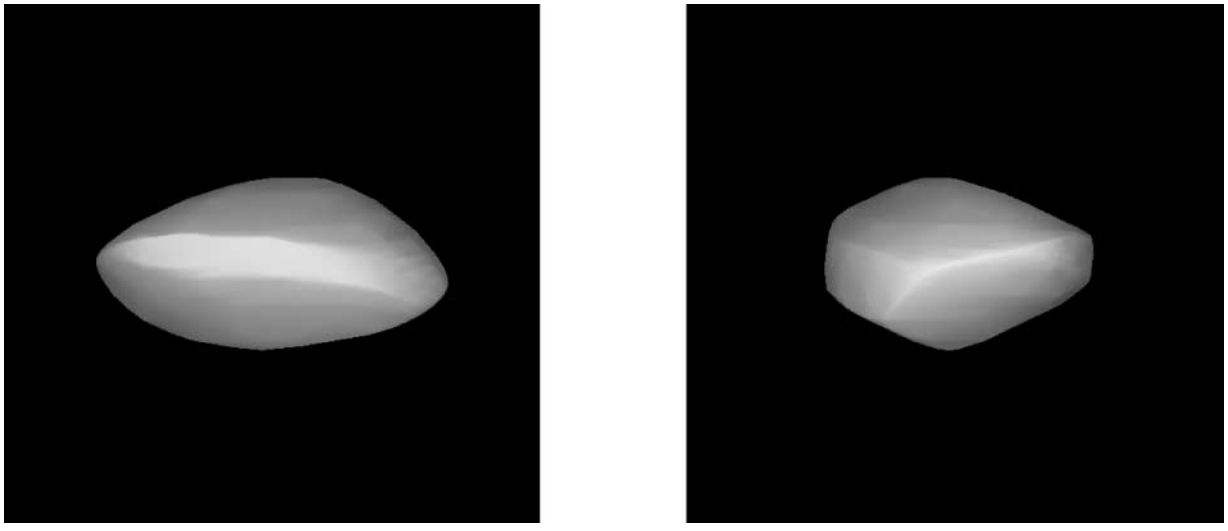

FIG. 23. The shape model of 45 Eugenia.

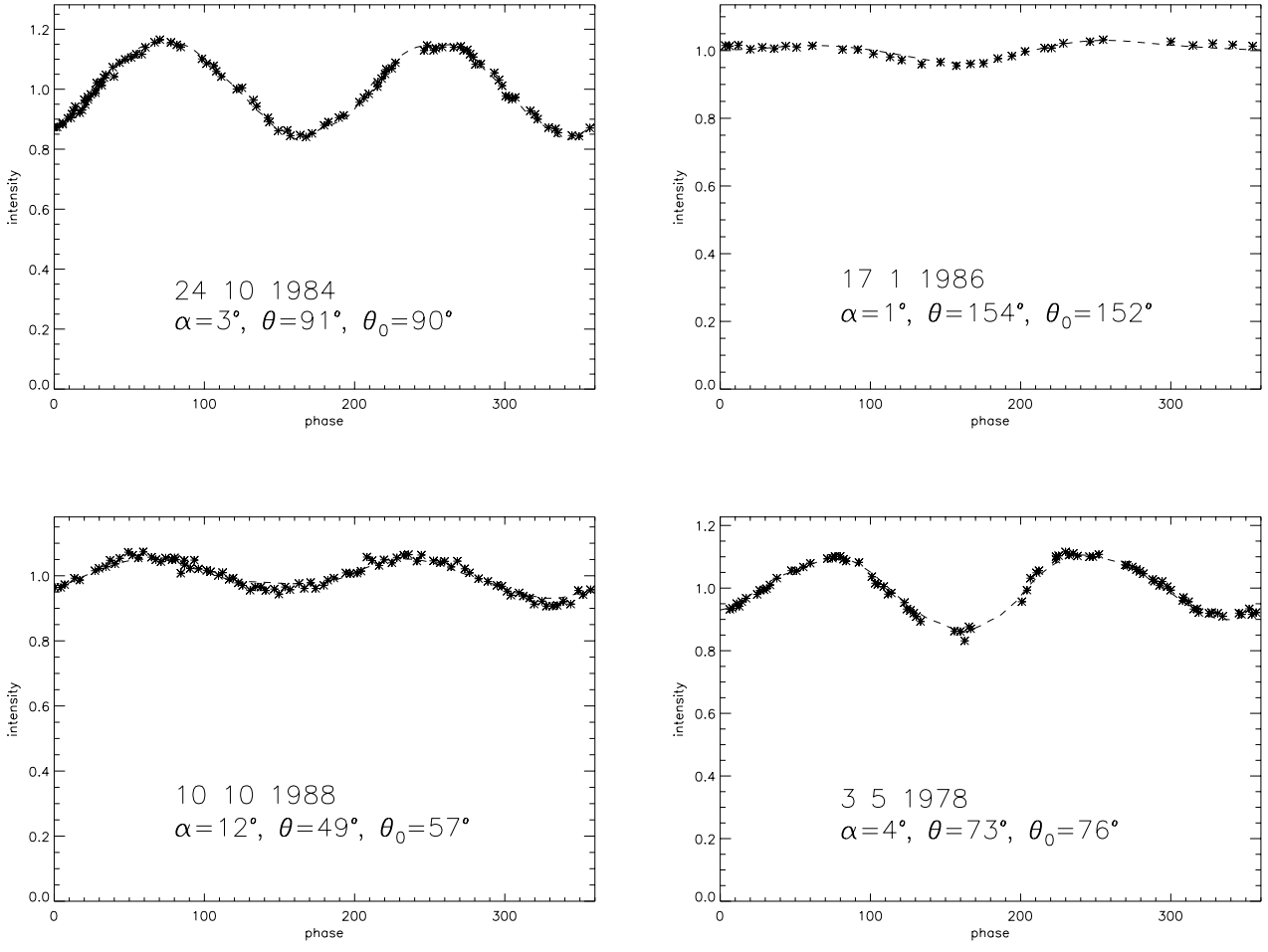

FIG. 24. Four lightcurves and the corresponding fits for 45 Eugenia.

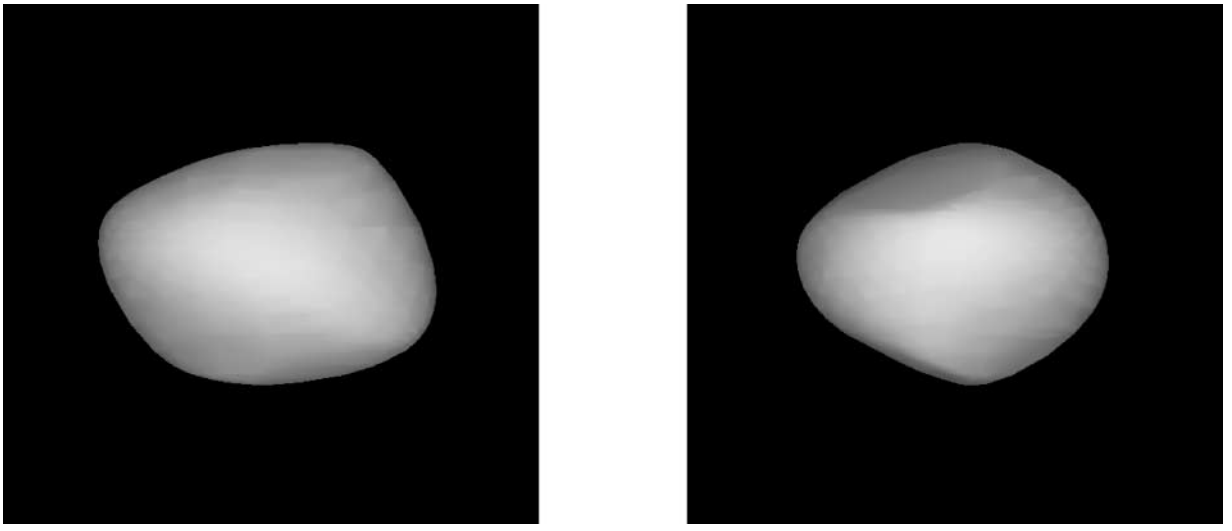

FIG. 25. The shape model of 52 Europa.

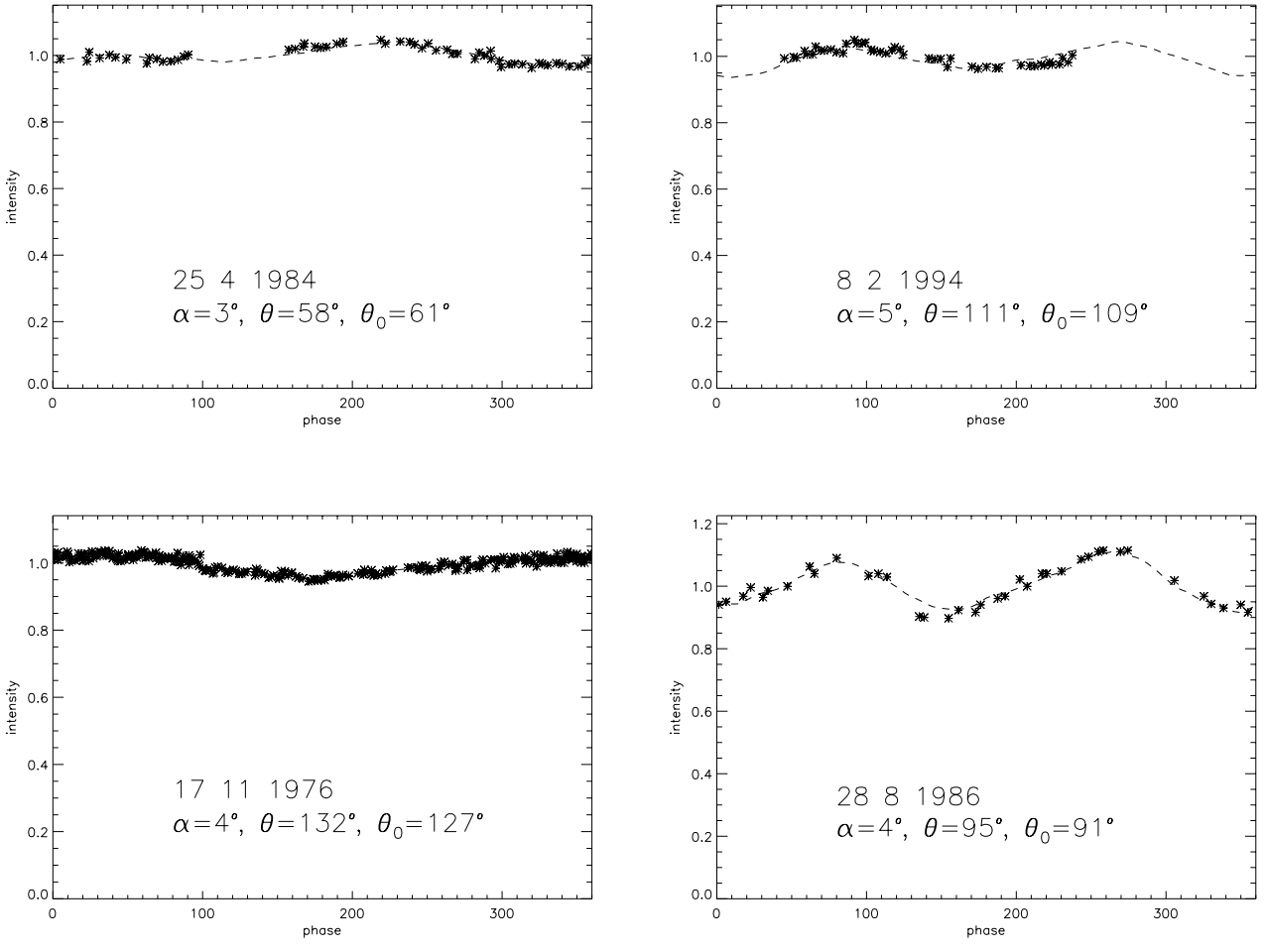

FIG. 26. Four lightcurves and the corresponding fits for 52 Europa.

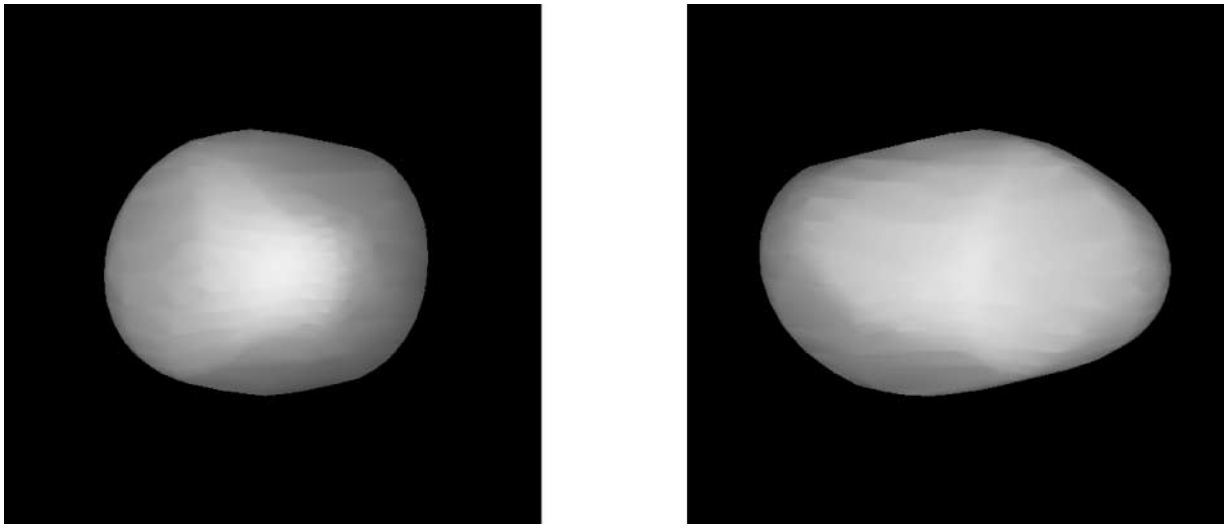

FIG. 27. The shape model of 87 Sylvia.

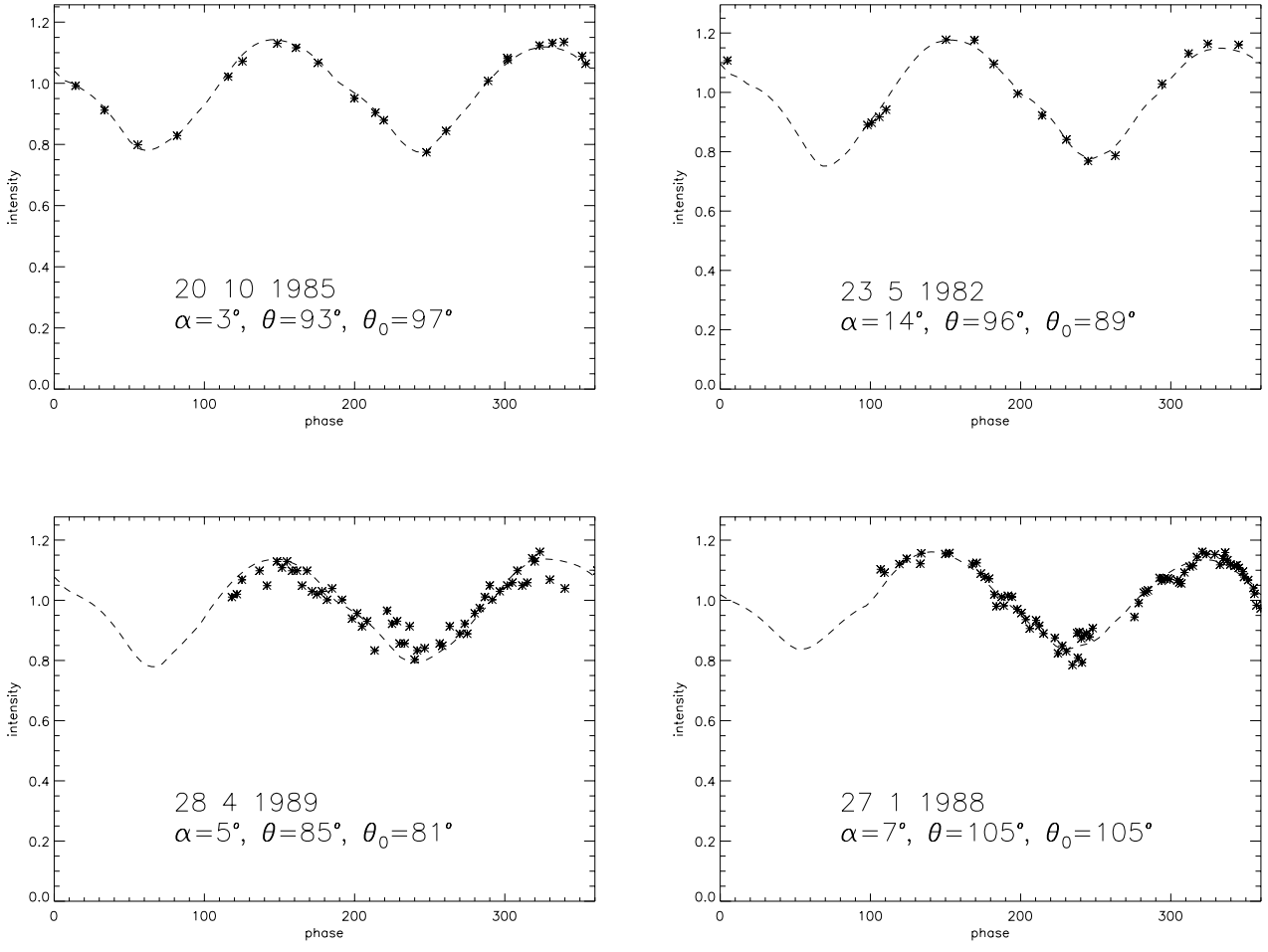

FIG. 28. Four lightcurves and the corresponding fits for 87 Sylvia.

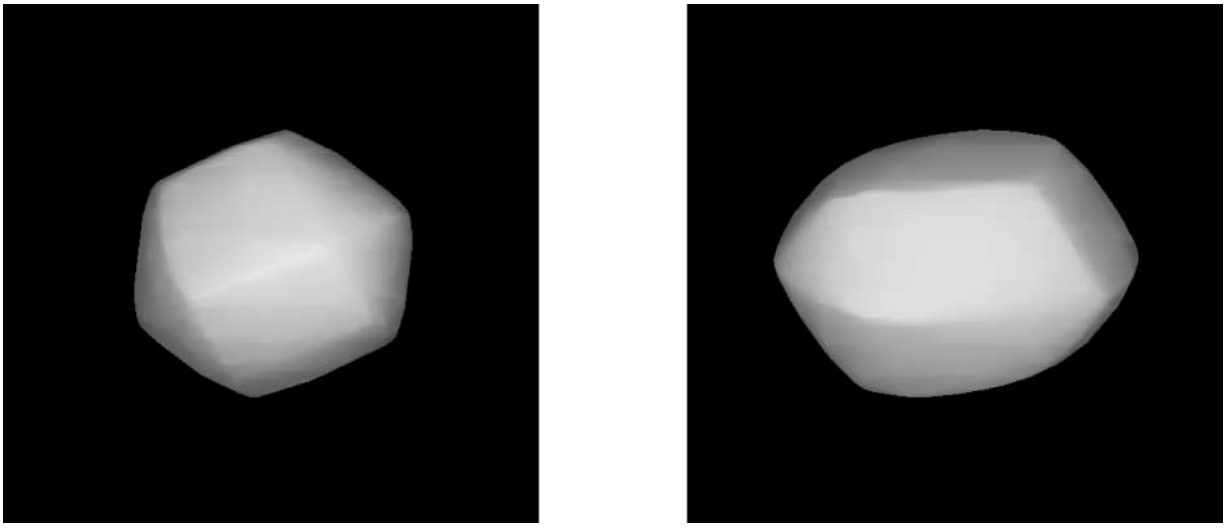

FIG. 29. The shape model of 192 Nausikaa.

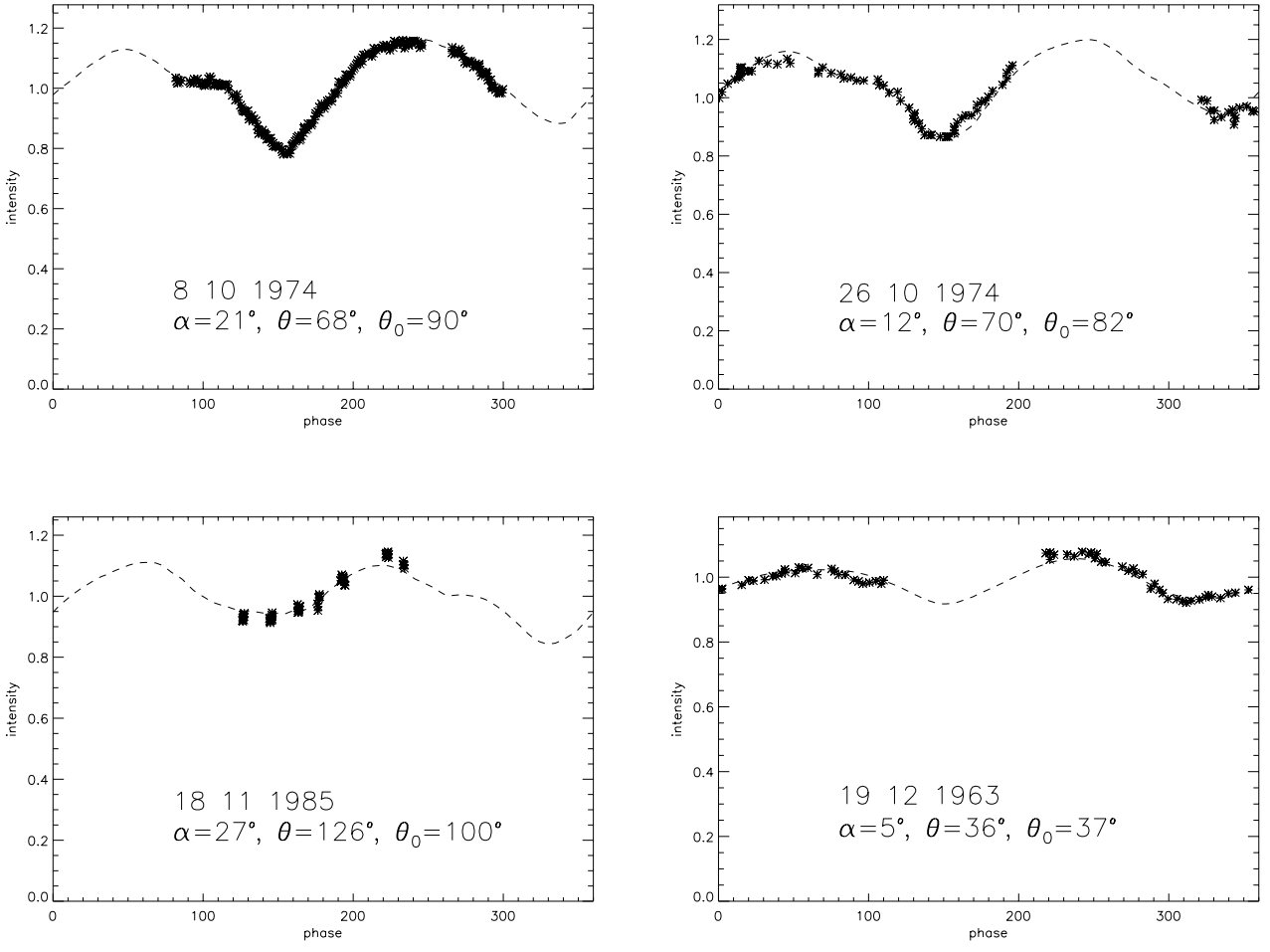

FIG. 30. Four lightcurves and the corresponding fits for 192 Nausikaa.

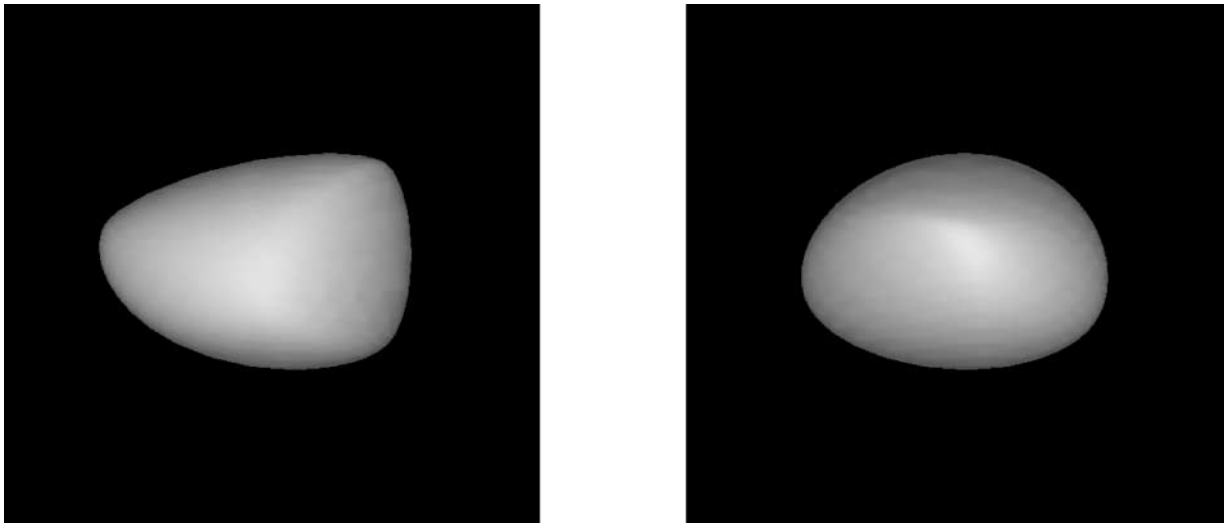

FIG. 31. The shape model of 354 Eleonora.

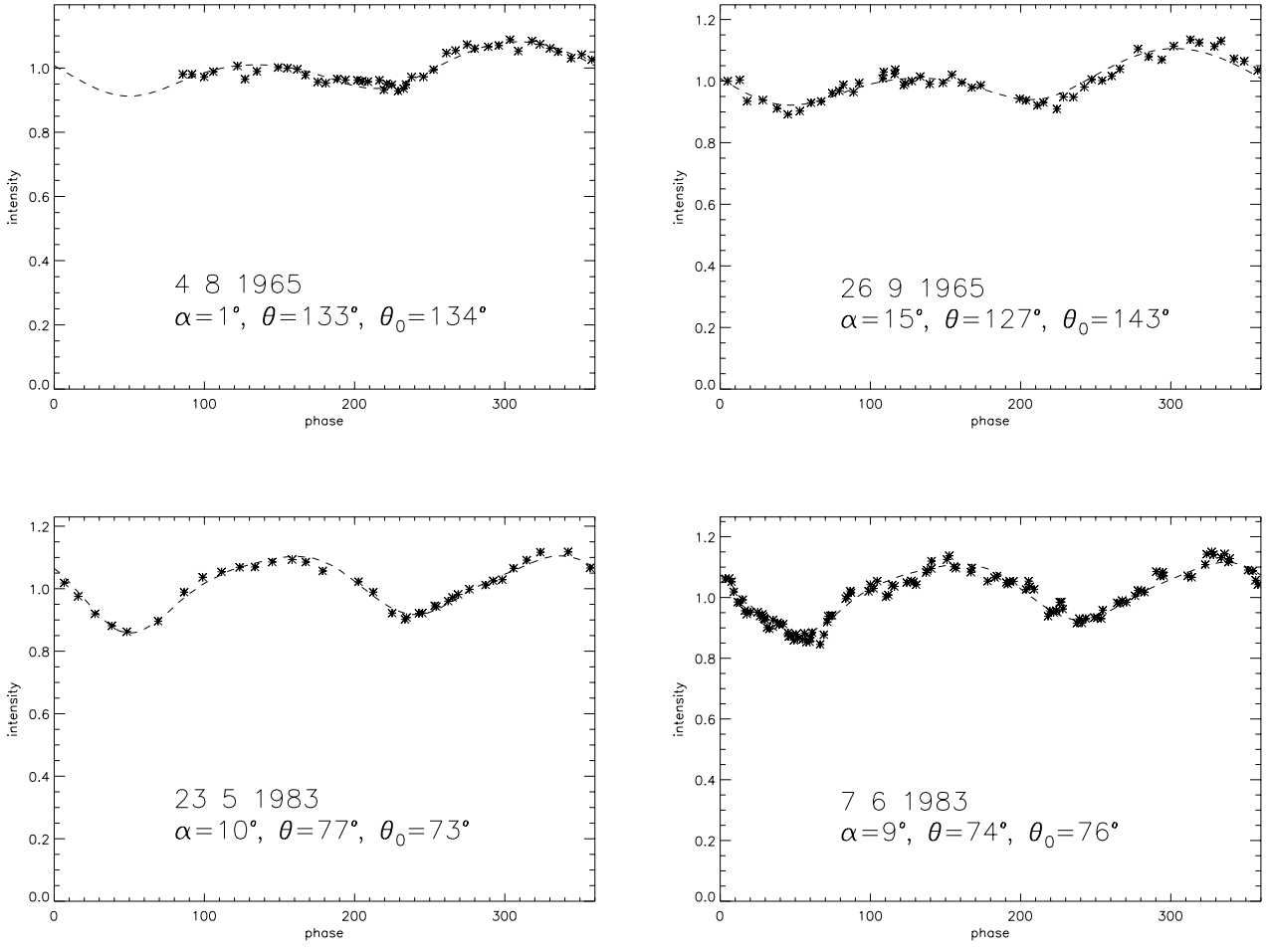

FIG. 32. Four lightcurves and the corresponding fits for 354 Eleonora.

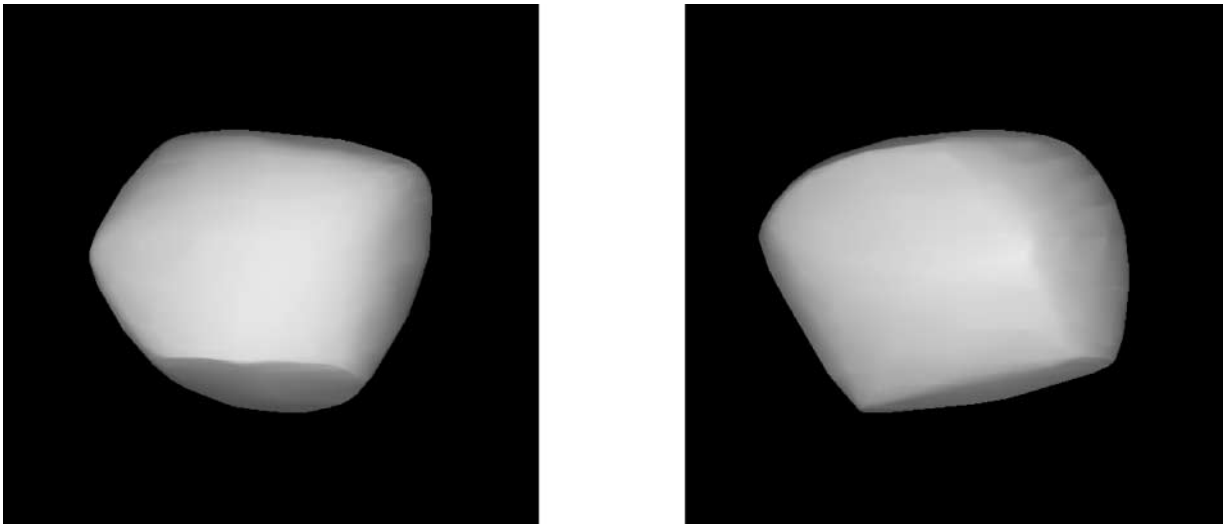

FIG. 33. The shape model of 532 Herculina.

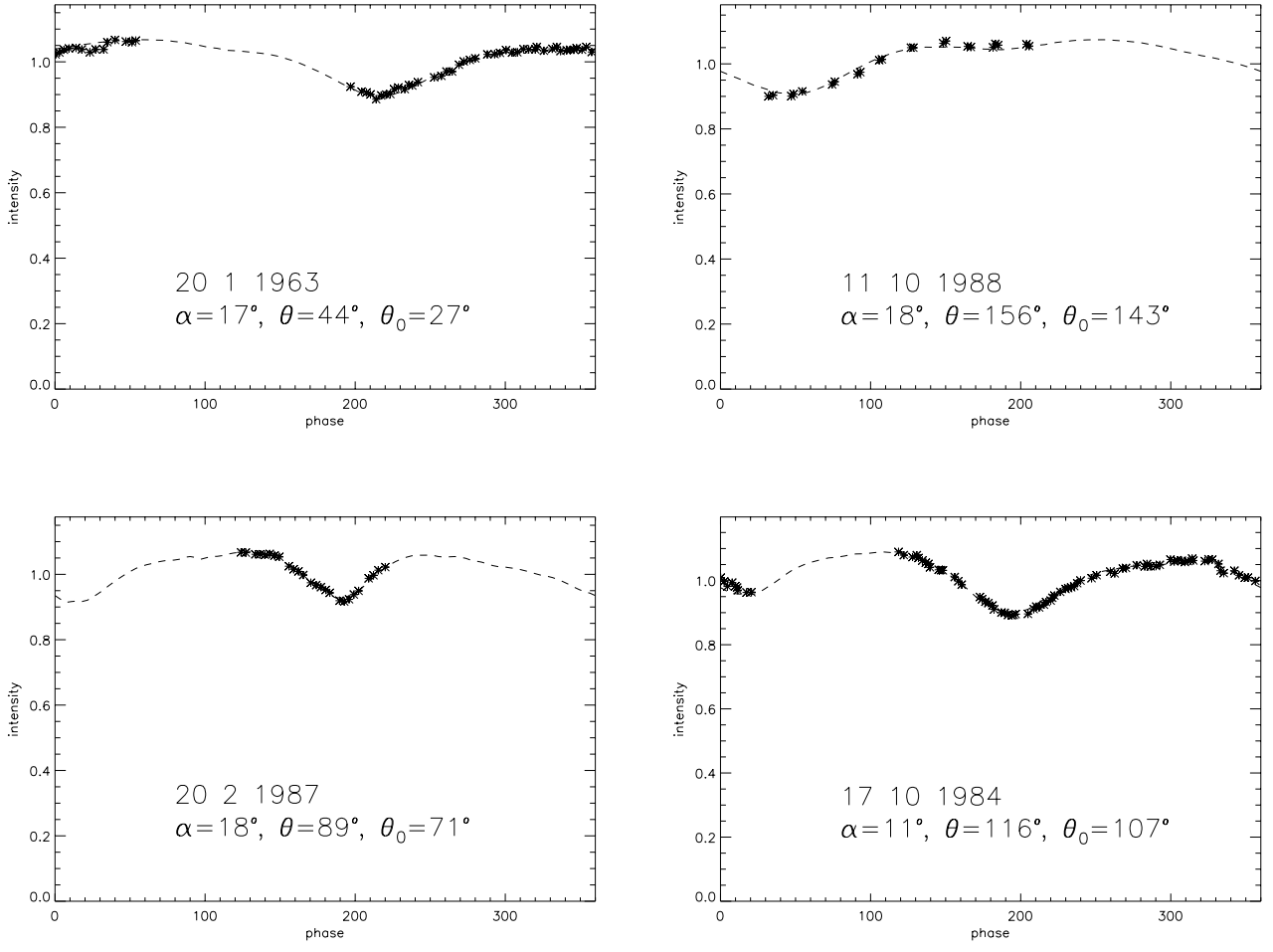

FIG. 34. Four lightcurves and the corresponding fits for 532 Herculina.

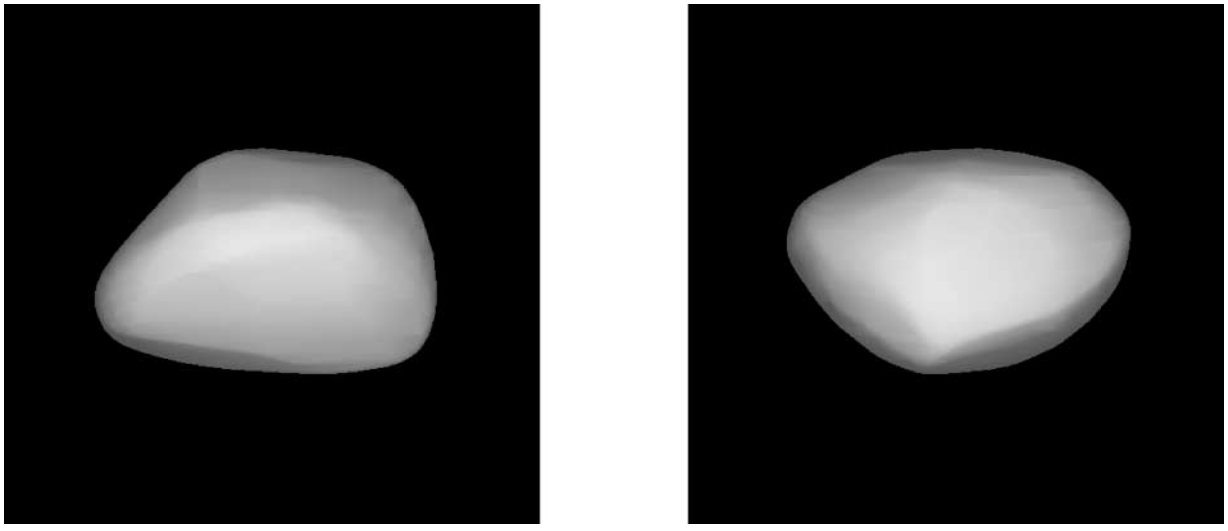

FIG. 35. The shape model of 1036 Ganymed.

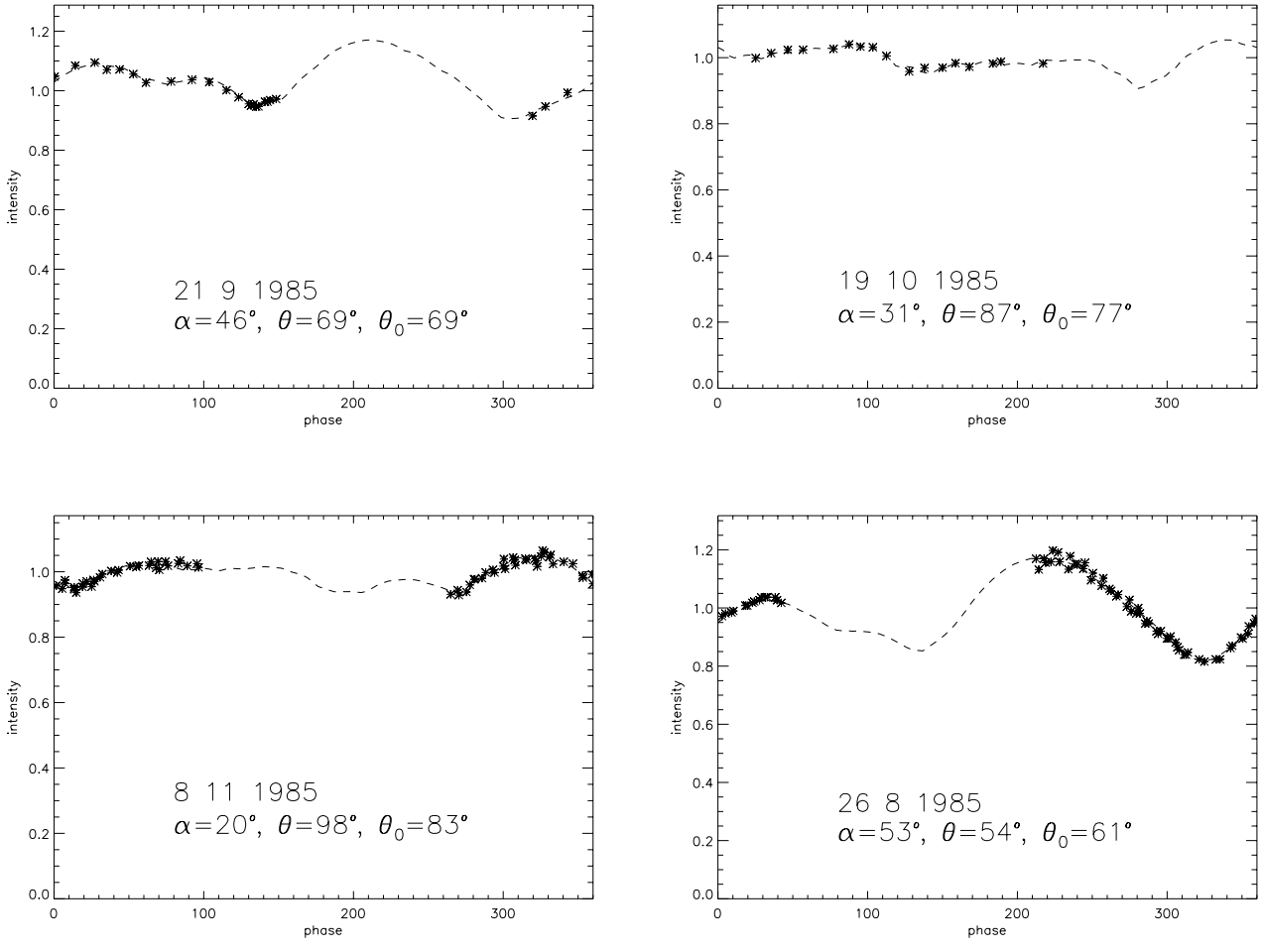

FIG. 36. Four lightcurves and the corresponding fits for 1036 Ganymed.

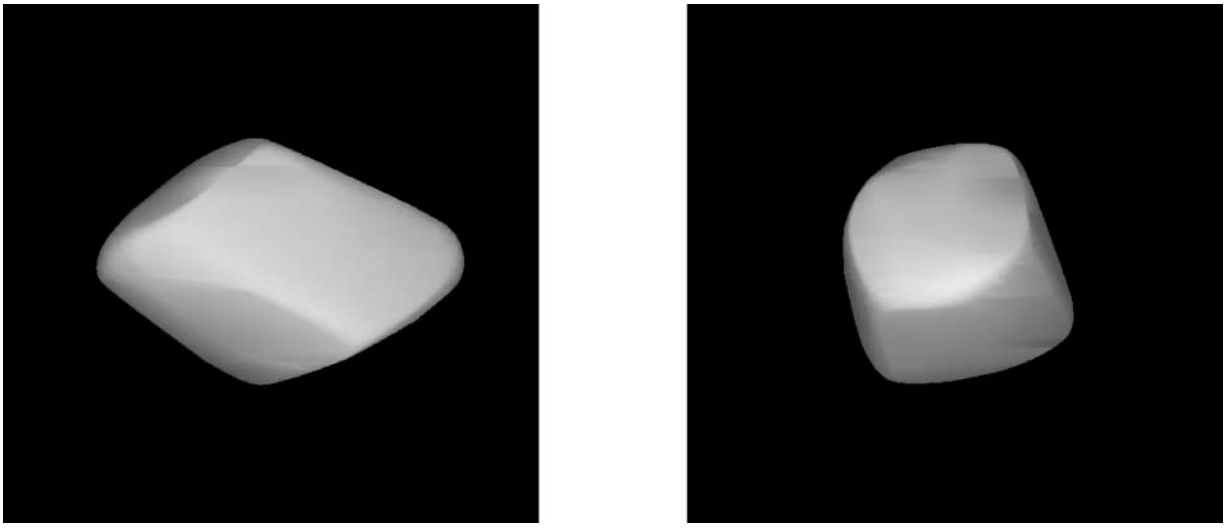

FIG. 37. The shape model of 3103 Eger.

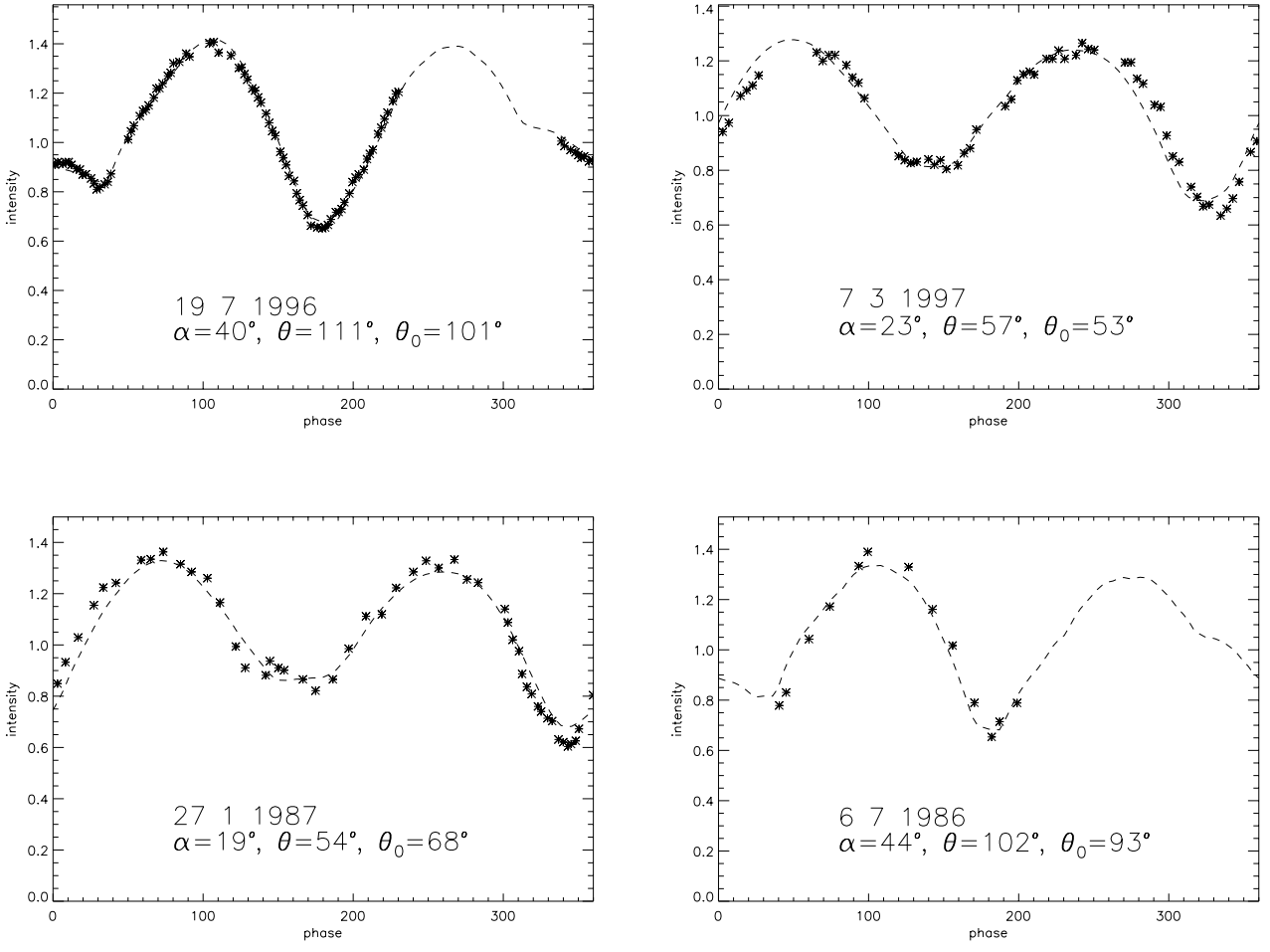

FIG. 38. Four lightcurves and the corresponding fits for 3103 Eger.

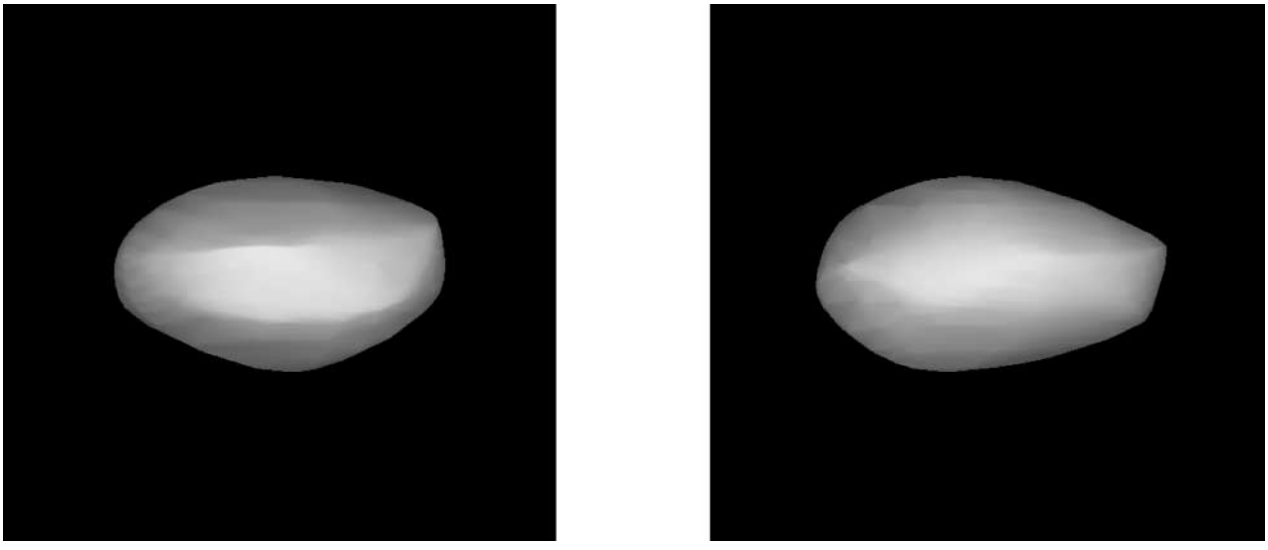

FIG. 39. The shape model of 6053 1993BW3.

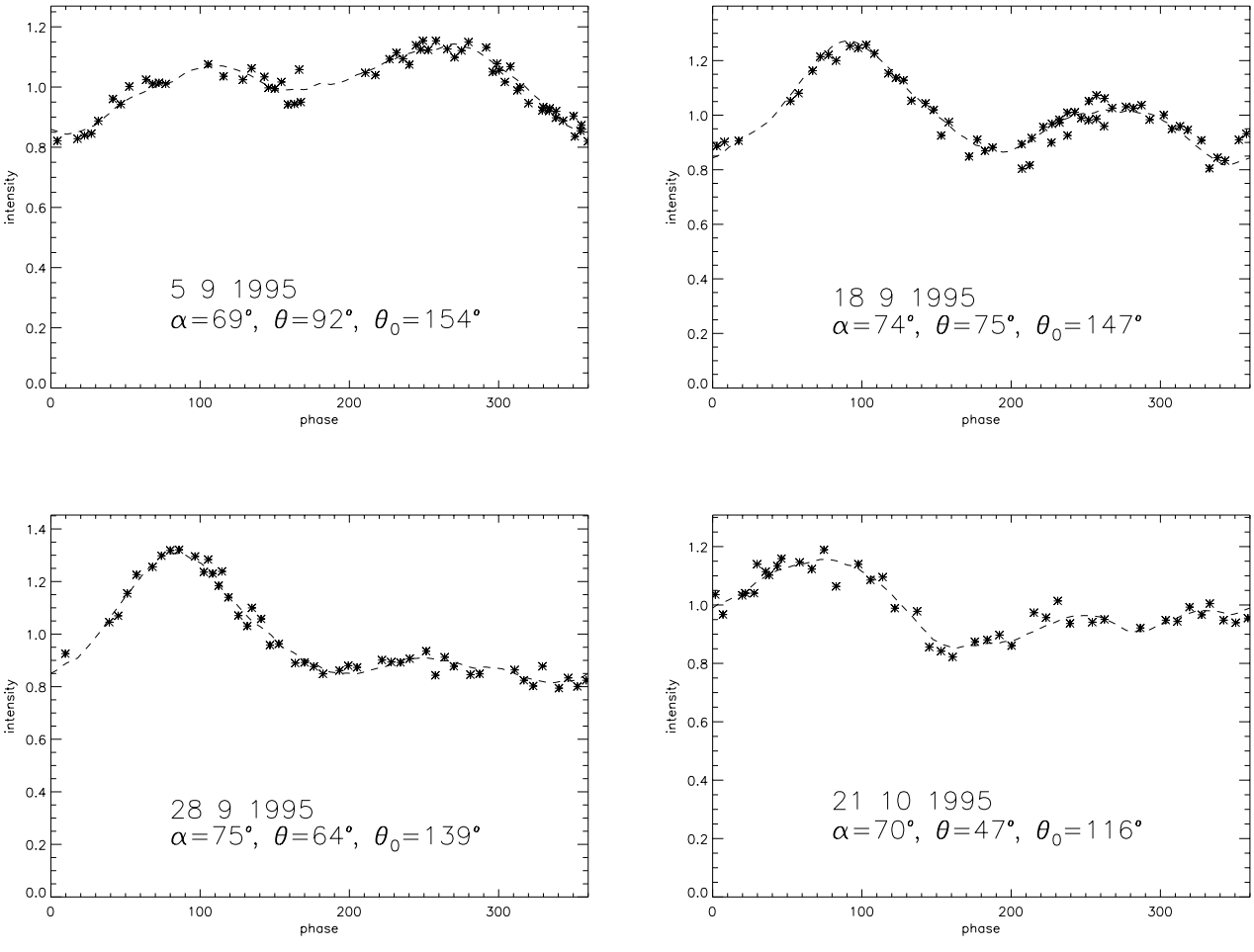

FIG. 40. Four lightcurves and the corresponding fits for 6053 1993BW3.

1036 Ganymed (Figs. 35 and 36). Ganymed (S-type, 40 km) is characterized by a somewhat anvil-like shape. Slight albedo variegation was detected, but it does not indicate a sizable albedo feature. The crude dimensions are $a/b = 1.0$, $b/c = 1.5$. The adopted pole seems to stand out from the other possibilities.

3103 Eger (Figs. 37 and 38). Eger is probably a 10-km-size object. The solution for the rotational state stood apart from the other possibilities, but its accuracy cannot be better than some $\pm 10^\circ$. The corresponding shape is quite irregular and slightly elongated, characterized by $a/b = 1.5$, $b/c = 1$. Some of the lightcurves feature the flat/sharp-minima phenomenon which is characteristic of a strongly asymmetric shape (cf. 44 Nysa in Kaasalainen *et al*. 2002). Considerable concavities are possible. The data set and the number of adequately different observing geometries were so limited that we can only call the model preliminary; we chose Eger as an example of pushing the inversion procedure to its limits. Another effect of minimal data is that the data set nominally allowed another pole solution wholly unconnected with the one mentioned, but the corresponding shape would have been in a clearly unphysical rotational state.

6053 1993BW3 (Figs. 39 and 40). This small near-Earth object was well observed during its 1995–1996 apparition, resulting in a good set of lightcurves at various observing geometries. The lightcurve features are easily explained by an irregular shape with dimensions about $a/b = 1.1$, $b/c = 1.6$, but there are two pole solutions, neither of which can honestly be said to be better than the other. One solution ($\beta = -8^\circ$, $\lambda = 358^\circ$) gives a slightly better fit for the shapes of the lightcurves, while the other one ($\beta = +10^\circ$, $\lambda = 178^\circ$) produces just slightly smaller offset errors for the absolute magnitudes of the lightcurves. Normally we would not give very much weight to the latter fact, but in this case the observations are all from one source, so the scattering among the absolute values can perhaps be expected to be smaller than usual. In any case, the shape results are rather similar, as with 16 Psyche. We portray the shape corresponding to the first pole; it is slightly more flattened than the other one.

5. CONCLUSIONS AND DISCUSSION

Our results reveal a variety of shapes; some smaller asteroids have angular features suggestive of collisional history. Many large asteroids display considerable irregularities as well, although their relative scale is smaller. Viewed collectively, this sample seems to corroborate physical expectations, i.e., the increase of irregularities and global-scale deviations from simple shapes as the body size decreases. Very few asteroids show evidence of global albedo variegation; even quite complex lightcurve features at rather small solar phase angles can be explained with an irregular shape. The intermediate-size and large asteroids in this sample can roughly be regarded as variations of ellipsoidal or potato shapes, even though these variations are sometimes considerable. The deformations are usually random-like and do not seem to indicate any particular global structure. However, we have found that a few other large asteroids such as 41 Daphne and 44 Nysa display clearly asymmetric shapes with global trends (Kaasalainen *et al*. 2002).

An essential part of lightcurve analysis is a reliable, regularly updated photometric data base. The UAPC is now being transformed into an automated service accessible via the Internet (Piironen *et al*. 2002). For modeling purposes (especially for main-belt asteroids), it is better to observe an object for which only a few more apparitions or less are needed rather than a new target. There are numerous such asteroids in the UAPC. As for NEAs, several lightcurves should be taken during an apparition—not just the customary one or two for rough period determination.

Since many of our models are based on more or less restricted data sets, further data may change, for example, the favoured pole solutions. These models should thus be considered evolving rather than fixed.

APPENDIX: ALBEDO SPOT MODELING

One of the advantages of convex modeling is the particular ease with which albedo models can be added to the shape if necessary. Denote the outward unit normal of a facet j of the model polyhedron by $\mathbf{n}_j$, and denote its facet value obtained in inversion (interpreted as the area of the facet possibly multiplied by an albedo value) by g_j. As described in KT, a residual vector

$$\mathbf{R} = \sum_j \mathbf{n}_j g_j \tag{1}$$

of size more than, say, 1% of the total area $\sum_j g_j$ of the model shape indicates significant albedo variegation. So far, we have found this to be the case only for a few asteroids.

If necessary, the albedo distribution can be modeled as one bright spot in the following way (a practical implementation of the approach outlined in KT). The direction of the vector $\mathbf{R}$ clearly implies the direction of surplus brightness, so all one needs to do is to determine the areas (and thus albedos) of the facets belonging to a spot of given size and centered in the surface normal direction of $\mathbf{R}$, such that the new sum (1) run over all facet areas vanishes. Since the problem is ambiguous, one can simply choose the first spot size that produces realistic (i.e., not too strong) albedo deviations from the unit value set for the facets outside the spot. Whether the spot radius is, say, 20° or 40° affects the shape very little, so the size and the resulting brightness of the spot are chosen mainly by visual judgment.

The unknown areas s_j of the M facets, the normals of which are within the given spot size (the rest of the facets have areas g_j), are obtained by minimizing

$$\chi^2_{\text{alb}} = \sum_{i=1}^{3} \left[R_i - \sum_{j=1}^{M} n_j^{(i)} (g_j - s_j) \right]^2 + \lambda_\varpi f(g/s), \tag{2}$$

and their albedos are then $\varpi_j = g_j/s_j$; Levenberg–Marquardt minimization (cf. KT) does the job robustly and in a flash. The regularization function f (with a suitable weight factor λ_ϖ) suppresses erratic deviation of facet albedos from each other. For example, an f measuring the albedo differences between adjacent facets produces a smooth and natural-looking brightness variation across the spot, whereas an f measuring the deviation of the facet albedos from the spot's average value produces as uniform a brightness over the spot as possible. To ensure positive facet areas, one should optimize the parameter a_j in $s_j = \exp(a_j)$ rather than the area itself. One could just as well model a dark spot in the direction opposite to the bright one; however, spacecraft data indicate that bright spots are more probable (especially for asteroids already covered by very dark material).

We emphasize the fact that the spot model is necessarily very vague: The foremost purpose of the model is to extract the shape solution as reliably as possible. (This solution is considerably more stable than the albedo one.)

ACKNOWLEDGMENTS

We thank Per Magnusson for a useful list of summarized versions of the previous models of UAPC asteroids and Josef Durech for valuable discussions. This research is funded, in part, by the Academy of Finland.

REFERENCES

Bowell, E., B. Hapke, D. Domingue, K. Lumme, J. Peltoniemi, and A. W. Harris 1989. Application of photometric models to asteroids. In *Asteroids II* (R. P. Binzel, T. Gehrels, and M. S. Matthews, Eds.), pp. 524–556. Univ. of Arizona Press, Tucson.

Brown, M. E., and J. L. Margot 2001. s/2001 (87). *IAU Circ.* 7588.

Helfenstein, P., and J. Veverka 1989. Physical characterization of asteroid surfaces from photometric analysis. In *Asteroids II* (R. P. Binzel, T. Gehrels, and M. S. Matthews, Eds.), pp. 557–593. Univ. of Arizona Press, Tucson.

Kaasalainen, M. 2001. Interpretation of lightcurves of precessing asteroids. *Astron. Astrophys.* **376**, 302–309.

Kaasalainen, M., and J. Torppa 2001 (KT). Optimization methods for asteroid lightcurve inversion. I. Shape determination. *Icarus* **153**, 24–36.

Kaasalainen, M., J. Torppa, and K. Muinonen 2001. Optimization methods for asteroid lightcurve inversion. II. The complete inverse problem. *Icarus* **153**, 37–51.

Kaasalainen, M., J. Torppa, and J. Piironen 2002. Binary structures among large asteroids. *Astron. Astrophys.* **383**, L19–L22.

Lagerkvist, C.-I., J. Piironen, and A. Erikson 2001 (UAPC). *Asteroid Photometric Catalogue*, 5th update. Uppsala Univ. Press, Uppsala.

Margot, J. L., and M. E. Brown 2001. s/2001 (22). *IAU Circ.* 7703.

Merline, W. J., and F. Menard 2001. s/2001 (22). *IAU Circ.* 7703.

Merline, W. J., and 9 colleagues 1999. Discovery of a moon orbiting the asteroid 45 Eugenia. *Nature* **401**, 565–568.

Piironen, J., C.-I. Lagerkvist, J. Torppa, M. Kaasalainen, and B. Warner 2001. Standard Asteroid Photometric Catalogue. *Bull. Am. Astron. Soc.* **33**, 1562.